1 **Inter-comparison of online and offline methods for measuring ambient heavy and trace elements**
2 **and water-soluble inorganic ions (NO$_3^-$, SO$_4^{2-}$, NH$_4^+$ and Cl$^-$) in PM$_{2.5}$ over a heavily polluted**
3 **megacity, Delhi**

4 Himadri Sekhar Bhowmik[1], Ashutosh Shukla[1], Vipul Lalchandani[1], Jay Dave[2], Neeraj Rastogi[2], Mayank

5 Kumar[3], Vikram Singh[4], and Sachchida Nand Tripathi[1*]

6 [1] Department of Civil Engineering, Indian Institute of Technology Kanpur, Kanpur, India

7 [1*] Department of Civil Engineering and Centre for Environmental Science and Engineering, Indian

8 Institute of Technology Kanpur, Kanpur, India

9 [2] Geosciences Division, Physical Research Laboratory, Ahmedabad, India

10 [3]Department of Mechanical Engineering, Indian Institute of Technology Delhi, New Delhi, India

11 [4]Department of Chemical Engineering, Indian Institute of Technology Delhi, New Delhi, India

12 *Correspondence to:* S. N. Tripathi (snt@iitk.ac.in)

13 Keywords: Aerosol mass spectrometer (AMS), Xact 625i ambient metal mass monitor, Ion
14 Chromatography (IC), ICP-MS, elemental composition.

15 **Abstract**

16 Characterizing the chemical composition of ambient particulate matter (PM) provides valuable information

17 on the concentration of secondary species, toxic metals and assists in the validation of abatement

18 techniques. The chemical components of PM can be measured by sampling on filters and analysing them

19 in the laboratory or using real-time measurements of the species. It is important for the accuracy of the PM

20 monitoring networks that measurements from the offline and online methods are comparable and biases are

21 known. The concentrations of water-soluble inorganic ions (NO$_3^-$, SO$_4^{2-}$, NH$_4^+$ and Cl$^-$) in PM$_{2.5}$ measured

22 from the 24 hrs filter samples using ion chromatography (IC) were compared with the online measurements

23 of inorganics from aerosol mass spectrometer (AMS) with a frequency of 2 mins. Also, the concentrations

24 of heavy and trace elements determined from the 24 hrs filter samples using inductively coupled plasma

25 mass spectroscopy (ICP-MS) were compared with the online measurements of half-hourly heavy and trace

26 metal's concentrations from Xact 625i ambient metal mass monitor. The comparison was performed over

27 two seasons (summer and winter) and at two sites (Indian Institute of Technology, Delhi and Indian Institute

28 of Tropical Meteorology, Delhi) which are located in characterized by their different metrological

29 ~~conditions at IITD and during winter at IITMD, two sites located in~~ Delhi, NCR, India, one of the heavily

30 polluted urban areas in the world. Collocated deployments of the instruments helped to quantify the

31 differences between online and offline measurements and evaluate the possible reasons for positive and

32 negative biases. The slopes for $SO_4^{2-}$ and $NH_4^+$ were closer to 1:1 line during winter and decreased during

33 summer at both sites. The higher concentrations on the filters were due to the formation of particulate

34 $(NH_4)_2SO_4$. Filter-based $NO_3^-$ measurements were lower than online $NO_3^-$ during summer at IITD and

35 winter at IITMD due to the volatile nature of $NO_3^-$ from the filter substrate. Offline measured $Cl^-$ was

36 consistently higher than AMS derived $Cl^-$ during summer and winter at both sites. Based on their

37 comparability characteristics, elements were grouped under 3 categories. The online element data were

38 highly correlated ($R^2 > 0.8$) with the offline measurements for Al, K, Ca, Ti, Zn, Mn, Fe, Ba, and Pb during

39 summer at IITD and winter at both the sites. The higher correlation coefficient demonstrated the

40 precision of the measurements of these elements by both Xact 625i and ICP-MS. Some of these

41 elements showed higher Xact 625i elemental concentrations than ICP-MS measurements by an average of

42 10-40% depending on the season and site. The reasons for the differences in the concentration of the

43 elements could be the distance between two inlets for the two methods, line interference between two

44 elements in Xact measurements, sampling strategy, variable concentrations of elements in blank filters and

45 digestion protocol for ICP measurements.

46 **1. Introduction**

47 The adverse effect of ambient particulate matter (PM) on human health and the role of PM in visibility

48 degradation, altering earth's radiation balance, and climate change has received global attention in the last

49 two decades (Pope et al., 2009; Hong et al., 2019; Wang et al., 2019). To gain better insight into their

50 properties, the chemical characterization of particulate matter and its source attribution is crucial. The

51 National Capital Region (NCR), which includes India's capital (New Delhi) along with some districts

52 (Gurugram, Faridabad, and Noida) of the adjoined states of Haryana, Rajasthan, and Uttar Pradesh, is one

53 of the most polluted urban areas in northern India with a population over 47 million (Bhowmik et al., 2021).

54 According to World Economic Forum, New Delhi was listed as the most polluted city globally, with an

55 annual average $PM_{2.5}$ concentration of ~140 µg m$^{-3}$ (World Health Organisation, 2018).  NCR has been a

56 specific area for researchers for the past couple of years due to its unprecedented $PM_{2.5}$ levels. Various large

57 and small scale industries, power plants, construction activities, and rapid increase in the vehicle numbers

58 (11 million in 2018) (Rai et al., 2020) are among the several causes that massively reduces the air quality

59 index (AQI) (Rai et al., 2020; Sharma & Kulshrestha, 2014). Further, the crop residue burning during the

60 month of Oct-Nov in the adjoining states of Haryana and Punjab on a larger scale worsens the air quality.

For decades, the mass concentrations of major water soluble inorganic ions (WSIS) and heavy and trace metals in PM have been carried out by sampling them on filters and subsequently analysing them in laboratory. Water-soluble inorganic ions (WSIS) and heavy and trace elements from these filter samples are analyzed using ion chromatography (IC) (Bhowmik et al., 2021; Rengarajan et al., 2007; Rastogi & Sarin, 2005) and inductively coupled plasma-mass spectroscopy (ICP-MS) or inductively coupled plasma-optical emission spectroscopy (ICP-OES) (Patel et al., 2021) respectively. Usually, these filters are collected over 24 hrs interval. Traditional receptor models usually use these offline measured data of very low temporal resolution, making it challenging to characterize the short pollution episodes and dynamics of pollution sources. Further, un-denuded filter sampling can have both negative and positive artifacts due to volatile species (Lipfert, 1994; Pathak & Chan, 2005). The absorption of acidic and alkaline gases on the filter substrates, if not removed prior to sampling, can give positive artifacts and result in overestimating species concentration. Likewise, the evaporation of semi-volatile compounds (ammonium nitrate) from filter substrates can give negative biases and result in underestimating aerosol concentration and its species (Pathak & Chan, 2005; X. Zhang & Mcmurryt, 1992). The degree of artifacts can be affected by several factors, including temperature, relative humidity, type of filter substrate, the aerosol loading on the filter substrate, etc. Transient events can also lead to mismatch. To overcome the limitations of low temporal resolution and avoid the artifacts associated with offline filter sampling, methods have been developed for measuring aerosol chemical composition at a higher time resolution in the order of hours or minutes.

Aerosol Mass Spectrometer (AMS) (Canagratna et al., 2007; Jayne et al., 2000; Jimenez et al., 2003) is one kind of such instrument, which provides size-resolved chemical composition of non-refractory submicron aerosols, e.g., organics, sulphate, nitrate, ammonium, and chloride at the order of hours or even minutes. For other important components, such as calcium (main constituents of soil dust and construction activities) and potassium (tracer of biomass burning), which AMS cannot measure, Xact ambient metal mass monitor can be used. It is capable of measuring 4540 elements, e.g., Al, Si, P, S, Cl, K, Ca, Ti, V, Cr, Mn, Fe, Co, Ni, Cu, Zn, Ga, Ge, As, Se, Br, Rb, Sr, Y, Zr, Nb, Mo, Pd, Ag, Cd, In, Sn, Sb, Te, I, Cs, Ba, La, Ce, Pt, Au, Hg, Tl, Pb and Bi with a frequency of every 30 mins to 4 hours. However, the high time-resolution instruments measure lower range of species concentrations with higher limit of detection (LOD) than the offline based methods (Tremper et al., 2018). Both offline and online methods have their own strength and weaknesses. Uncertainties in offline filter analysis methods have been extensively studied (Pathak & Chan, 2005; Viana et al., 2006), but the novel online methods pose new problems (Wu & Wang, 2007). For example, when the ambient concentrations are very low, online measurements are often close to the MDL values due to the short integration times (Malaguti et al., 2015).

93     Previous studies in Delhi-NCR have used low time resolution filter-based methods for chemical
94     characterization of submicron aerosols (Bhowmik et al., 2020; Nagar et al., 2017; Pant et al., 2015; S. K.
95     Sharma et al., 2016; Singhai et al., 2017). On the other hand, there are only a few studies in Delhi-NCR
96     that used high time resolution methods (HR-ToF-AMS, Q-ACSM, Xact) for characterization and source
97     apportionment of coarse and fine particulate matters (Gani et al., 2019; Lalchandani et al., 2021; Rai et al.,
98     2020, 2021; Singh et al., 2021; Tobler et al., 2020). Online and offline measurements both have their
99     advantages and limitations. For both these measurements, the quality of the data highly depends on the
100    calibration of the instruments. For Xact, the multi-element mix standard might not represent ambient
101    elemental mix if the ambient particulate matters are too low or too high in concentration, affecting the
102    collection properties of the filter (Indresand et al., 2013). For filter-based water-soluble inorganic ion and
103    metal analysis, confidence in the data depends on the calibration as well as the volatility, solubility, and
104    digestion protocol used for the extraction of water-soluble inorganic ions and elements, respectively. Thus,
105    it is vital for monitoring networks that both the offline and online measurement methods give comparable
106    results. Few published studies have compared inorganics and elements from filter-based measurements and
107    semi-continuous methods (e.g., Furger et al., 2017; Nie et al., 2010). The inter-comparison in these studies
108    is unjustified for highly polluted areas, as the specie values observed in these studies are much below MDL
109    due to very low ambient concentration of secondary species and elements. It will be interesting to study the
110    inter-comparison in highly polluted areas. To the best of our knowledge, there are neither any published
111    seasonal and temporal comparisons of inorganics from high time resolution AMS measurements and filter-
112    based measurements from ion chromatography nor any comparisons of heavy and trace metals from high
113    time resolution Xact 625 ambient metal mass monitor and offline measurements from ICP-MS in the
114    heavily polluted Delhi NCR region.

115    This study demonstrates a comparison between online and offline measurements of WSIS and heavy and
116    trace metals at two sites in Delhi NCR during summer (June-July 2019), characterized by moderate levels
117    of local pollution and winter (October-December 2019), affected by high levels of pollution from local
118    sources and regional transport of crop residue burning emissions from adjoining state of Haryana and
119    Punjab.

120    **2. Methodology**

121    **2.1. Sampling sites**

122    Delhi-NCR, a highly polluted urban area with an annual average $PM_{2.5}$ concentration of 140 μg m$^{-3}$ and a
123    population of over 47 million, is surrounded by the Thar desert on its west and Indo-Gangetic Plain on its

124    east to south-east. The temperature is about ~35°C-48°C during summer (April-June), and winter

125    (December-February) is relatively cooler, with temperature ranges from ~2°C-15°C (Bhowmik et al., 2020;

126    Vipul Lalchandani et al., 2021; Tobler et al., 2020). The wind is mostly north-westerly during both summer

127    and winter.

128
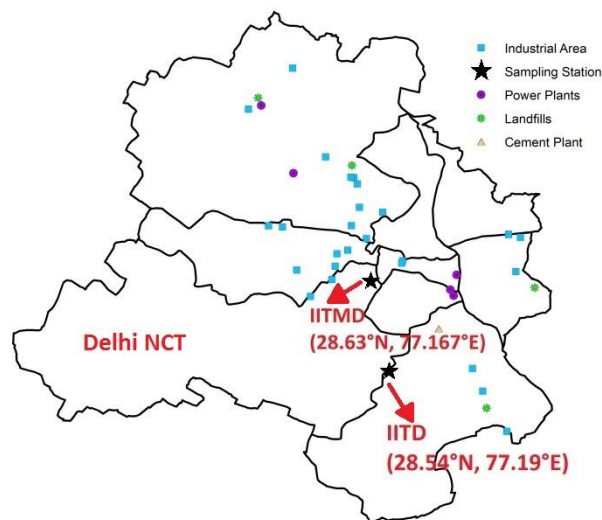
129        Fig.1. Sampling sites with various emission sources like power plants, industries, landfills, etc.

## 2.1.1. Delhi NCR site 1: IITD

131    High volume $PM_{2.5}$ samples were collected on the rooftop of the Centre for Atmospheric Science (CAS)

132    building at the Indian Institute of Technology, Delhi (IITD) (28.54°N, 77.19°E; ~218 m amsl) about ~15

133    m above the ground level. Further, one HR-ToF-AMS and Xact ambient metal mass monitor were deployed

134    inside a temperature-controlled laboratory on the 3$^{rd}$ floor of the same building about ~10 m above the

135    ground level. It is an educational institute cum as well as residential campus having restaurants nearby and

136    very close to (<200 m) heavy traffic road. Lalchandani et al., (2021); Rai et al., (2020) observed source

137    signatures of emissions from industries, power plants, vehicles, and waste burning in this site.

## 2.1.2. Delhi NCR site 2: IITMD.

139    Offline $PM_{2.5}$ sampling was carried out on the rooftop of the main building at the Indian Institute of Tropical

140    Meteorology Delhi (IITMD) (28.63°N, 77.167°E; ~220 m above msl) about 15 m above the ground level.

141    Moreover, HR-ToF-AMS and Xact ambient metal mass monitor were installed inside a temperature-

142    controlled laboratory on the 2$^{nd}$ floor of the same building at the height of ~8 m from the ground level. This

site is placed in the central urban area of Delhi and surrounded by Central Ridge reserve forest and residential areas (Tobler et al., 2020) and around 14 km away in North West direction from IITD. A recent study by Lalchandani et al. (2021) observed the site is dominated by emissions from traffic, solid fuel burning, and oxidized organic aerosols. The location of the sampling sites are shown in Fig. 1.

## 2.2. Sampling details

### 2.2.1 Offline sampling

Biweekly 24 hrs (January- September 2019) and daily 24 h (October- December 2019) $PM_{2.5}$ samples were collected on quartz filter substrates (Whatman; $8 \times 12$ inches) using a high-volume sampler (HVS) with a flow rate of 1.13 $m^3$/min. Blanks were collected in the field by placing a fresh filter in the sampler while not running. A total of 64 filters (60 from IITD site during June-July 2019 including 4 blanks) were collected in summer whereas, a total of 186 filters (90 from each site during October-December 2019 plus 6 blanks) were collected in winter. The collected filters, including field blanks, were zip-locked and stored in the freezer at each site and periodically transported to CESE (Centre for Environmental Science and Engineering), IIT Kanpur, where they were further stored at -20˚C in a deep freezer prior to analysis. For this study, the samples from the common period of offline and online sampling (October-December 2019) from the two sites were analyzed for WSIS ($SO_4^{2-}$, $NO_3^-$, $NH_4^+$ and $Cl^-$) using an IC, and 32 metals (Al, Na, K, Ca, Ti, V, Cr, Mn, Fe, Ni, Cu, Zn, As, Se, Rb, Sr, Zr, Cd, Sn, Sb, Ba, Pb, Cs, La, Ce, Pt, Tl, Mg, Li, Mo, Co and Pd) using an ICP-MS. More details of analytical procedures are given in the instrumentation section.

### 2.2.2 Online sampling

At both IITD and IITMD site, high-resolution time-of-flight aerosol mass spectrometers (HR-ToF-AMS, Aerodyne Research Inc., Billerica, MA) (Canagaratna et al., 2007; DeCarlo et al., 2006), equipped with $PM_{2.5}$ aerodynamic lens (Peck et al., 2016) (Aerodyne Research Inc., Billerica, MA, USA) were installed inside air-conditioned laboratories. Ambient fine particulate matters were sampled through $PM_{2.5}$ cyclone (BGI, Mesa Labs. Inc.) inlet at IITD with a flow rate of 5 lpm (l/min) using a 2.44 m long stainless-steel tubing (0.3 inch I.D and 0.4 inch O.D) and through black silicon tubing (0.19 inch O.D) at IITMD, placed 1.5 m above the rooftop. A Nafion dryer (MD-110-144P-4: Perma Pure, Halma, UK) was used to dry the ambient aerosols to maintain the output RH at 20%. At both IITD and IITMD site, high-resolution time-of-flight aerosol mass spectrometers (HR-ToF-AMS, Aerodyne Research Inc., Billerica, MA) (Canagaratna et al., 2007; DeCarlo et al., 2006), equipped with $PM_{2.5}$ aerodynamic lens (Peck et al., 2016) (Aerodyne Research Inc., Billerica, MA, USA) were installed. Ambient fine particulate matters were sampled through

173 ~~PM$_{2.5}$ cyclone (BGI, Mesa Labs. Inc.) inlet at IITD and through black silicon tubing at IITMD, placed ~1.5-~~
174 ~~2 m above the rooftop with a flow rate of 5 l/min using long stainless-steel tubing (12 mm O.D). An aerosol~~
175 ~~sample dryer system (Aerodyne research, Inc) was used to dry the ambient aerosols to maintain the output~~
176 ~~RH at 20%.~~ At IITD, data were collected from 12$^{th}$ October 2019-31$^{st}$ December 2019 and 2$^{nd}$ June 2019-
177 21$^{st}$ July 2019 during winter and summer campaigns respectively. The data between 1$^{st}$ November and 14$^{th}$
178 November was not available, due to hardware issues in the AMS during that period. At IITMD, data were
179 only collected during winter campaign from 25$^{th}$ October 2019 to 31$^{st}$ December 2019.

180 Two Xact 625i ambient metal monitors (Cooper Environmental Services, Beaverton, Oregon, USA) were
181 installed inside temperature controlled laboratories at IITD and IITMD. Ambient aerosols were sampled
182 through a PM$_{2.5}$ inlet with a flow rate of 16.7 lpm. A separate sampling line of 2.44 meter (1.25 inch I.D)
183 for the Xact which was made of aluminium was installed. A heater was set up at the end of the sampling
184 line to ensure 45% RH set point. At IITD, sampling was carried out from 1$^{st}$ October 2019-31$^{st}$ December
185 2019 and 30$^{th}$ May 2019-25$^{th}$ July 2019 during the winter and summer campaign, respectively. However,
186 data between 16$^{th}$ July and 24$^{th}$ July were not available due to hardware breakdown. At IITMD, samples
187 were collected from 1$^{st}$ October 2019-31$^{st}$ December 2019 but data from 18$^{th}$ November to 26$^{th}$ November
188 2019 and 30$^{th}$ November to 14$^{th}$ December 2019 were not available due to instrumental problems.

189 Online measurements of inorganic ions (SO$_4^{2-}$, NO$_3^-$, NH$_4^+$ and Cl$^-$) from HR-ToF-AMS were compared
190 with the WSIS using an IC. Parallelly, heavy and trace metals obtained from Xact ambient metal mass
191 monitor were compared with the metal data from the offline filter measurements using an ICP-MS. Though
192 the sampling periods of AMS, Xact, and HVS were different for different seasons and different sites as well
193 (Table 1), only the common periods of online and offline sampling have been discussed in this study for
194 comparison.

195 Table 1. Sampling strategy and instrumentation used.

|  | Interval | IITD | IITMD |
|---|---|---|---|
| **Quartz filter Sampling** | 3 days | January-September 2019 | January-September 2019 |
|  | 24 hrs | October-December 2019 | October-December 2019 |
| **HR-Tof-AMS** | 2 mins | 2$^{nd}$ June-21$^{st}$ July 2019 | 25$^{th}$ October-31$^{st}$ December 2019 |
|  |  | 12$^{nd}$ October-31$^{st}$ December 2019 |  |
| **Xact** | 30 mins | 30$^{th}$ May-25$^{th}$ July 2019 | 1$^{st}$ October-31$^{st}$ December 2019 |
|  |  | 1$^{st}$ October-31$^{st}$ December 2019 |  |

196     Filters from the common periods were analysed for WSIS and heavy and trace metals using an IC and ICP-MS respectively.

## 197    2.3. Instrument details

## 198    2.3.1 WSIS measurements by IC and HR-ToF-AMS

199    For WSIS analysis, 9 sq.cm punch area of each collected filter was soaked in 30 ml of high purity milli-q
200    water (resistivity-18.20 M$\Omega$ cm) for 12 hours in pre-cleaned borosilicate test tubes to ensure maximum
201    solubility. The amount of water added, soaking time, etc. effect the solubility of the ions as well as the
202    extent of extraction. Details can be found in our previous paper (Bhowmik et al., 2020). Soaked samples
203    were filtered through 0.22 µm quartz filter papers to remove any suspended contaminations after an
204    ultrasonication for 50 mins. $Cl^-$, $NO_3^-$, $SO_4^{2-}$ and, $NH_4^+$ were measured for all the filter extracts by an IC
205    (Metrohm 883 Basic IC plus for cations and 882 compact IC plus for anions). Separate columns for the
206    analysis of cations and anions were installed in two separate modules. For anion and cation separation, an
207    AS 5-250/4.0 chromatography column and C-6 column was used, respectively. The sample carried by 3.2
208    mM $Na_2CO_3$+1 mM $NaHCO_3$ solution and 2.7 mM $HNO_3$ solution in the anion and cation module
209    separately passes through the charged columns to analyze each ion according to their polarity. The
210    calibration was performed by a seven-point method with a range of standards prepared by the serial dilution
211    from the stock solution standard of 10 ppm purchased from Metrohm. The uncertainty of the water-soluble
212    inorganic ions measured by IC was estimated as 4% (coverage factor~2) by the approach described in
213    Yardley et al. (2007).

214    HR-ToF-AMS measures size-resolved mass spectra of non-refractory particles (PM components that
215    vaporize at 600°C and $10^{-5}$ Torr, e.g., organics, nitrate, sulphate, ammonium, and some chlorides) of
216    submicron particulate matters. The details of this instrument can be found elsewhere (DeCarlo et al., 2006).
217    Briefly, ambient aerosols are collected through an orifice of 100 µm diameter and focused into a narrow
218    particle beam by an aerodynamic lens system installed inside the instrument, which has a transmission
219    efficiency of > 50% for $PM_{2.5}$ (DeCarlo et al., 2006; Peck et al., 2016). The particle size is determined after
220    analyzing the time of flight, i.e., time taken to travel along the length of the sizing chamber. The NR-PMs
221    are then vaporized by hitting the vaporizer at 600°C and at a vacuum of $10^{-7}$ Torr. Further, the vaporized
222    molecules are electronically ionized at 70 eV, followed by detection by a mass spectrometer as per their
223    *m/z*. HR-ToF-AMS can be operated in W-mode or V-mode. For this study, it was operated in V-mode with
224    a sampling time of 2 mins. Mass spectra (MS) mode, in which mass spectra of the components are
225    measured, and particle time-of-flight (PToF) mode in which the size-resolved mass spectra are measured,

226 are alternated in every 30s in 2 cycles. The HR-ToF-AMS was calibrated using standard protocols provided

227 in our previous publication (Lalchandani et al., 2021; Singh et al., 2019).

228 To determine the mass concentration of NR-PMs, Unit mass resolution (UMR) analysis was done using the

229 SQUIRREL data analysis toolkit (version 1.59) programmed in IGOR Pro 6.37 software (Wavemetrics,

230 Inc., Portland, OR, USA). High resolution (HR) analysis was also done on the data set using Peak Integrated

231 Key Analysis (PIKA version 1.19) toolkit. A recommended collection efficiency (CE) of 1 (Hu et al., 2017)

232 was used for capture vaporizer. At the beginning and mid of each campaign at the two sites, ionization

233 efficiency (IE) calibration was performed by injecting mono-disperse 300 nm ammonium nitrate and

234 ammonium sulphate particles into AMS and a condensation particle counter (Jayne et al., 2000). A relative

235 ionization efficiency (RIE) of 4.05 and 4.35 was used for IITD and IITMD site, respectively in case of $NH_4$.

236 RIE of $SO_4$ was taken as 2.89 and 1.67 for IITD and IITMD, respectively. For Org and Cl, by default a RIE

237 of 1.4 and 1.3 were taken, respectively. More details can be found in (Lalchandani et al., 2022). At the

238 beginning of each campaign at the two sites, ionization efficiency calibration was performed by injecting

239 mono-disperse 300 nm ammonium nitrate and ammonium sulphate particles into AMS and a condensation

240 particle counter (Jayne et al., 2000). More details can be found in Lalchandani et al. (2021) (manuscript

241 under review).

242 **2.3.2 Heavy and trace metal measurements by ICP-MS and Xact 625i**

243 For the analysis of heavy and trace metals, 15 sq. cm area of each collected filter was digested in an acid

244 mix of 0.5 ml HF+1.5 ml $HNO_3$ for 4 hours within closed HDPE Teflon tubes using a Hot plate (Savillex-

245 HF resistive Model number 88888:00000). The temperature range should be ~90-120˚C to ensure complete

246 digestion of the elements. Further, 2.5 ml of $HClO_4$ was added to the precipitates, left over the Teflon tube

247 wall and the tubes were kept on the hot plate at 220-240˚C for another 4 hours with the lids open for

248 complete evaporation of the acid mix. Moreover, the residual was dissolved in 6N $HNO_3$ and diluted with

249 de-ionized water (resistivity-18.20 MΩ cm) followed by filtering through 0.22 µm quartz filter papers prior

250 analysis. Details can be found in our forthcoming paper. This method is well established and used in many

251 studies (Minguillón et al., 2012; Querol et al., 2008).

252 Thirty two metals (Al, Na, K, Ca, Ti, V, Cr, Mn, Fe, Ni, Cu, Zn, As, Se, Rb, Sr, Zr, Cd, Sn, Sb, Ba, Pb, Cs,

253 La, Ce, Pt, Tl, Mg, Li, Mo, Co and Pd) were analyzed for all filter extracts using an ICP-MS (Thermo

254 Scientific iCAP Q ICP-MS) at IIT Kanpur Environmental Engineering laboratory. Si could not be

255 determined in the filter samples because Si is the primary constituent of the quartz filters and hence digested

256 during sample preparation. Samples were first introduced to a nebulizer using an injector attached to an

257 autosampler for transformation into fine aerosol droplets followed by ionization at a very high temperature

258 (8000K) in Ar-plasma. The elements elute as per their *m/z*. A known concentration (5 ppb) of Ge was used

259 as an internal standard to monitor the instrumental drift during the analysis. The overall average drift was

260 reported as $\pm$ 10%. The calibration was performed by ten-point method with a range of mix standards

261 prepared by the serial dilution from the High purity multi-element (35 elements) standards (soluble in 1%

262 $HNO_3$, 100 ppm) purchased from Sigma Aldrich.

263 The Xact 625i Ambient Metals Monitor (Cooper Environmental Services (CES), Beaverton, OR, USA)

264 uses X-ray fluorescence to measure the real-time elemental data in particulate matter. For this study, a $PM_{2.5}$

265 inlet was used. Details of the instrument can be found in Furger et al., 2017. Briefly, aerosol samples were

266 collected on a Teflon filter tape followed by hitting the loaded area with X-rays and the fluorescence

267 measured by a silicon drift detector (SDD). Thirty elements: Al, Si, S, Cl, K, Ca, Ti, Cr, Mn, Fe, Co, Ni,

268 Cu, Zn, As, Se, Br, Rb, Sr, Zr, Mo, Cd, In, Sn, Sb, Te, Ba, Pb, Bi, and Bi were measured with 30 min time

269 resolution. The Xact 625i was calibrated during each campaign using thin film standards for the individual

270 elements. The reproducibility was observed within $\pm$ 5%. Every midnight energy alignment checks were

271 performed for 15 mins (00:15 to 00:30) (for Cr, Pb, Cd and Nb). An uncertainty of ~10% was reported by

272 the manufacturer in an interference free situation (USEPA & Etv, 2012). This included 1.73% from flow

273 (CEN, 2014), 5% for standard reproducibility or uncertainty during calibration (USEPA, 1999) and 2.9%

274 from term stability as reported in Tremper et al. (2018). More details on the instrumental set up and stability

275 check during the summer and winter campaign can be found in Rai et al. (2020) and Shukla et al. (2021).

276 **3. Results and discussions**

277 **3.1. Online and offline measurements of WSIS and their comparison**

278 Large temporal variability was observed in both offline and online measurements of WSIS ($NO_3^-$, $SO_4^{2-}$

279 and, $NH_4^+$ and $Cl^-$) during the winter campaign and summer campaign at both sites. The inorganics data

280 with 2 mins interval from HR-ToF-AMS were averaged over the sampling period of the filters, i.e., 24

281 hours. The time series of $NO_3^-$, $SO_4^{2-}$, $NH_4^+$, and $Cl^-$ during the summer and winter campaign at IITD and

282 winter campaign at IITMD are shown in Fig. SM1 in the supplementary material. Higher peaks of

283 inorganics were observed during 25th Oct-18th Nov during the winter campaign at IITD, which was the

284 agricultural crop-residue burning period (Nagar et al., 2017). During the winter campaign, $NO_3^-$ was the

285 most abundant ion followed by $SO_4^{2-}$, $NH_4^+$ and $Cl^-$ for both offline and online measurements at both the

286 sites whereas, during the summer campaign at IITD, $NO_3^-$ was the most abundant ion followed by $NH_4^+$,

287 $SO_4^{2-}$ and $Cl^-$ in online measurement (HR-ToF-AMS). Similar results were observed in our companion

288  paper, Shukla et al. (2021). Interestingly, in the case of offline measurements during the summer campaign

289  at IITD, $NO_3^-$ was least abundant, and the sequence changed as $SO_4^{2-}> NH_4^+ >Cl^-> NO_3^-$. The average

290  concentrations with their ranges are tabulated in Table SM1 in supplementary material, and the mean,

291  maximum and minimum concentration are shown in Fig. 2 using box plots.

292  Comparability and correlation between offline and online measurements were evaluated in this study by

293  applying linear regression using offline data as the independent and online data as the dependent variable.

294  The comparability of $NH_4^+$ measurements was observed to be good for both summer and winter campaigns

295  at both sites. During the winter campaign, the correlations were $R^2=0.76$, and $R^2=0.89$, and the slopes were

296  closer to 1 (0.99 for IITD and 0.93 for IITMD) for IITD and IITMD, respectively (Fig. 3). Interestingly

297  during the summer campaign at IITD, though the correlation improves ($R^2=0.91$), the slope decreases to

298  0.49. This is likely because the vapor concentration of sulfuric acid ($H_2SO_4$) is negligible during winters

299  and higher during summers. As a result of which, the adsorption of sulfuric acid on PM deposited on the

300  filter papers happens during summers which react with gaseous ammonia ($NH_3$) to form a relatively stable

301  particulate $(NH_4)_2SO_4$ (D. Zhang et al., 2000), thus increasing ammonium concentration in the offline

302  measurements during the warmer season, especially in the presence of dust (Nicolás et al., 2009).

303

304

305
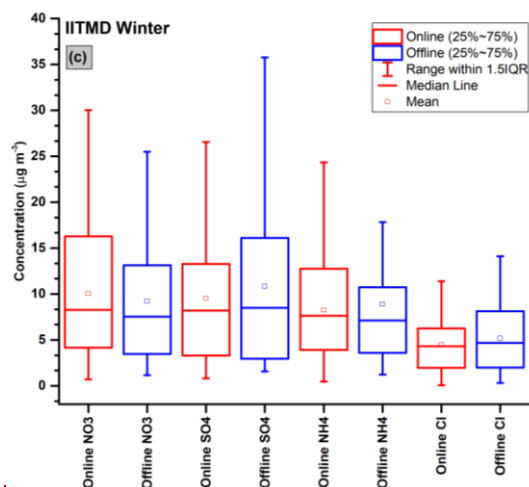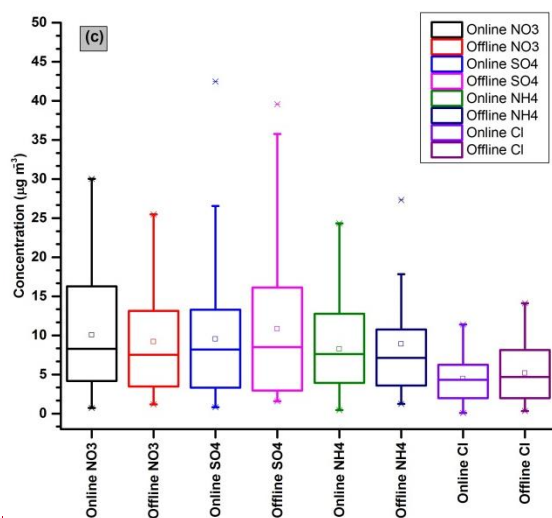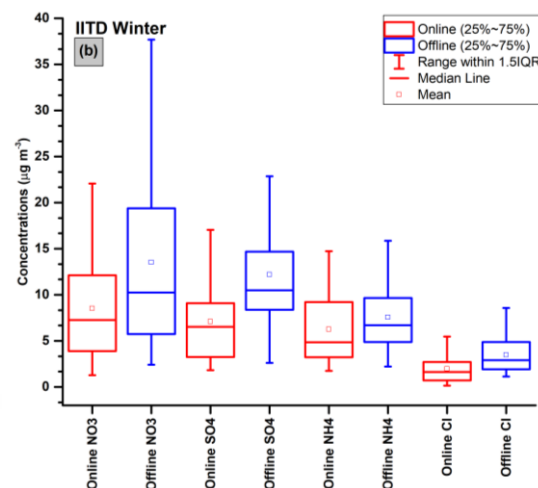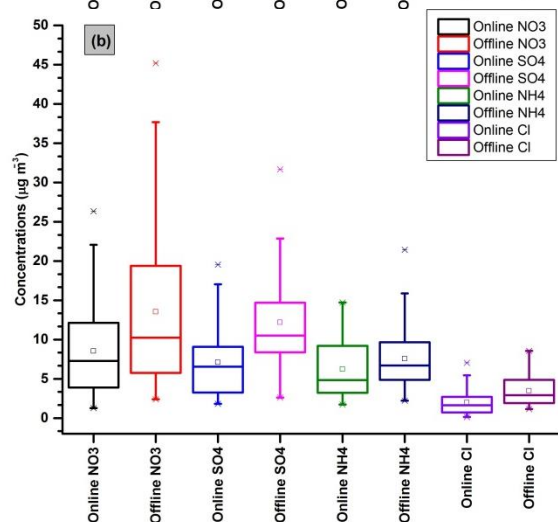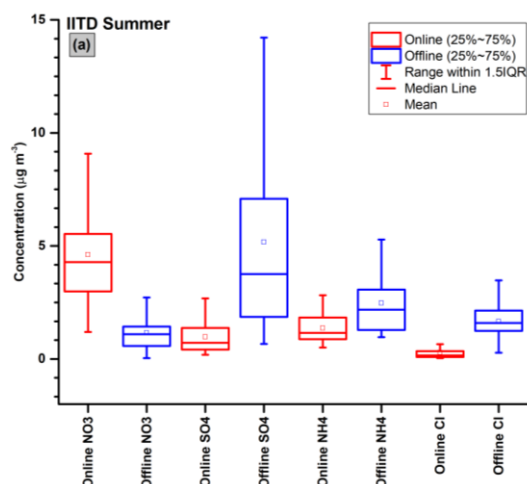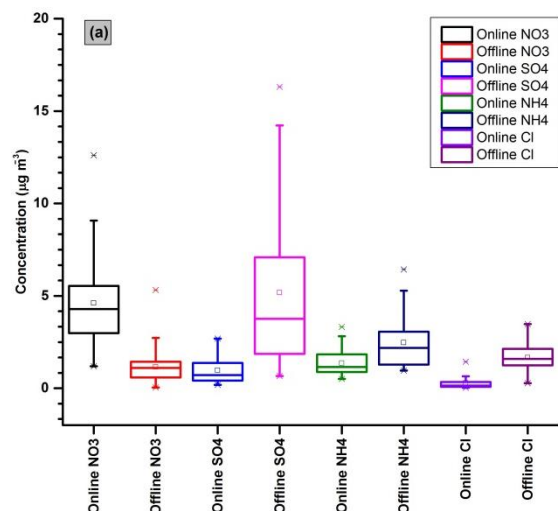
306 Fig.2. Box plots of online and offline measured secondary species ($NO_3^-$, $SO_4^{2-}$ and, $NH_4^+$) and $Cl^-$ during

307 (a) summer campaign at IITD, (b) winter campaign at IITD, and (c) winter campaign at IITMD site.

308 The filter-based measurements of $SO_4^{2-}$ were higher than those from the online measurements for IITD and

309 IITMD during both the seasons (Fig. 2). Their comparability is characterized by a correlation coefficient of

310 $R^2$=0.93 with a slope of 0.17 and $R^2$=0.82 with a slope of 0.68 at IITD during the summer and winter

311 campaigns, respectively. Interestingly, offline $SO_4^{2-}$ data correlates well with online $SO_4^{2-}$ data having a

312 correlation coefficient of $R^2$=0.93 with a slope close to 1 (0.93) during the winter campaign at IITMD (Fig.

313 3). A slope of less than 0.5 was observed in Malaguti et al., (2015) in Italy during the warm period whereas

314 the offline measurement of $SO_4^{2-}$ was 34% lesser than the AMS measurements in Pandolfi et al., (2014).

315 The higher $SO_4^{2-}$ concentrations on the un-denuded offline filter-based measurements could be due to

316 refractory sulfate (e.g., potassium or calcium sulfate). The higher filter-sulfate could also be possibly

317 because of the positive sampling artifact. The $SO_2$ is absorbed on the filter by the collected alkaline particles

318 (Nie et al., 2010). The higher concentration could also be due to the formation of ammonium bi-sulfate or

319 ammonium sulfate because of the reaction between gas-phase ammonia with the acidic aerosols (Nicolás

320 et al., 2009). Also, the un-denuded filter measurements could lead to higher filter-sulfate. The interaction

321 of gas phase ammonia with acidic aerosols can be minimized by using denuders while collecting aerosols

322 on the filters (Nault et al., 2020). Some studies suggested that the $NH_4$, $SO_4$ and, $NO_3$ measured by AMS

323 have interferences from organics and can often be misinterpreted as fully inorganic (Chen et al., 2019;

324 Farmer et al., 2010; Day et al., 2021). Though the interference is minimum, this could lead to possible

325 biases between the online and offline measurement of the inorganics. ~~The higher $SO_4^{2-}$ concentrations on~~

326 ~~the un-denuded offline filter-based measurements were possibly because of the positive sampling artifact.~~

327 ~~$SO_2$ is absorbed in the filter by the collected alkaline particles (Nie et al., 2010). The higher concentration~~

328 ~~could also be due to the formation of particulate $(NH_4)_2SO_4$ because of the earlier discussed reactions~~

329 ~~between gas phase $NH_3$ and $H_2SO_4$ formed on the fine particles (Nicolás et al., 2009).~~

330

331

332

333
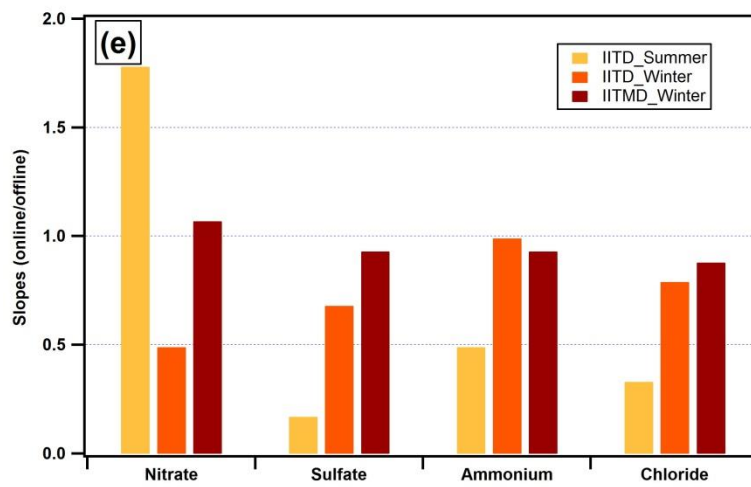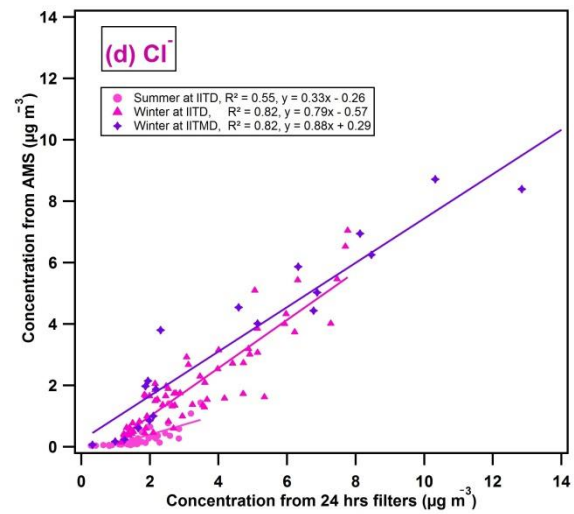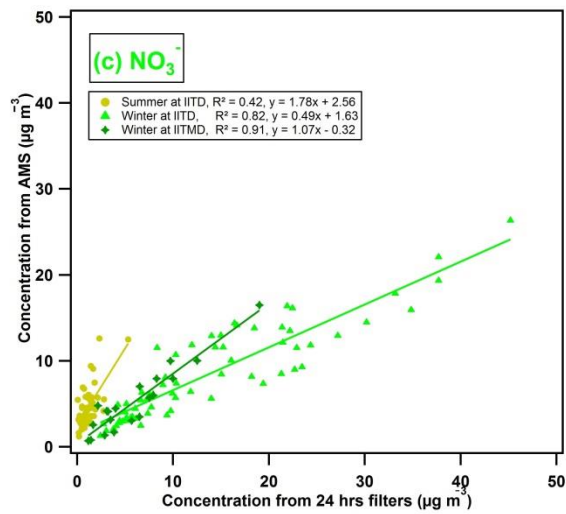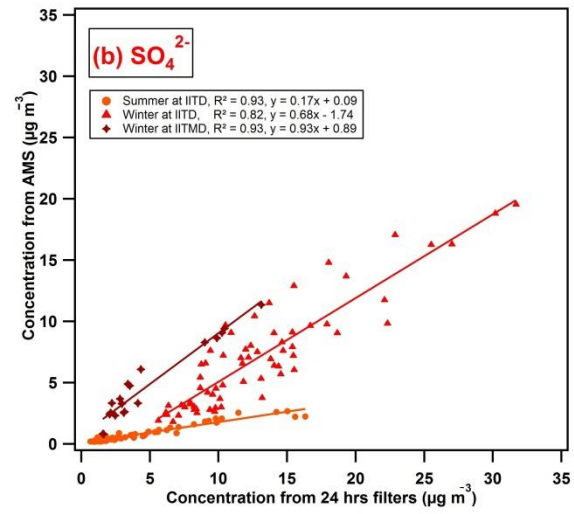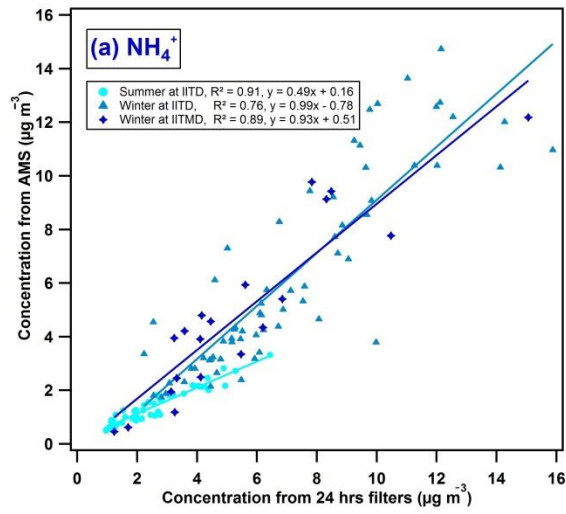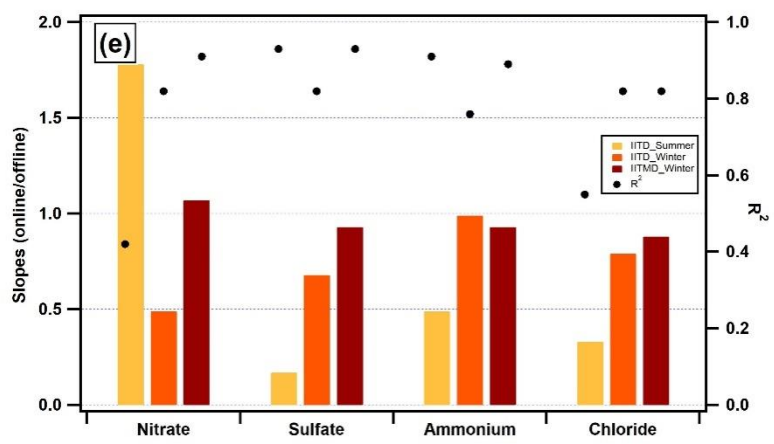
Fig.3. Scatter plots between online and offline measured (a) $NH_4^+$, (b) $SO_4^{2-}$, (c) $NO_3^-$, (d) $Cl^-$ concentrations and (e) comparison of slopes (online/offline) & $R^2$ of the measured inorganic ions in $PM_{2.5}$ during summer and winter campaign at IITD and during winter campaign at IIITMD.

~~The $NO_3^-$ concentrations measured by the HR-ToF-AMS were higher than the offline data during summer at IITD and during winter at IITMD whereas, filter-based measurements of $NO_3^-$ were higher during winter at IITD (Fig. 2).~~ The online and offline measurements posed a good correlation during winter ($R^2 = 0.91$ and slope of 1.07 at IITMD, $R^2 = 0.82$ and slope of 0.49 at IITD) whereas the correlation worsens during summer at IITD ($R^2 = 0.42$ and slope of 1.78) (Fig. 3). ~~The linearity worsens during summer at IITD ($R^2 = 0.42$ and slope of 1.78) (Fig. 3).~~ The slopes and correlation coefficient for the WSIS are listed in Table 2. The $NO_3^-$ concentrations measured by the HR-ToF-AMS were higher than the offline data during summer at IITD and during winter at IITMD whereas, filter-based measurements of $NO_3^-$ were higher during winter at IITD (Fig. 2). The higher offline $NO_3^-$ concentrations during winter at IITD can be possibly because of the positive artifact due to the absorption of gas-phase nitric acid ($HNO_3$) on the filter (Chow, 1995). ~~Pandolfi et al., (2014) observed $NO_3^-$ HR-AMS/Filter ratios of ~1.7 at Barcelona and Montseny in Europe. The higher offline $NO_3^-$ concentrations during winter at IITD can be possibly because of the positive artifact due to the absorption of gas-phase nitric acid ($HNO_3$) on the filter (Chow, 1995).~~ Many studies (Chow et al., 2008; Kuokka et al., 2007; Malaguti et al., 2015) reported higher concentrations of $NO_3^-$ from high time resolution measurements than filter-based measurements due to the evaporation of ammonium nitrate collected on filters over the duration of sample collection (Pakkanen & Hillamo, 2002; Schaap et al., 2004; Kuokka et al., 2007). Pandolfi et al. (2014) observed $NO_3^-$ HR-AMS/Filter ratios of ~1.7 at Barcelona and Montseny in Europe. This evaporation loss increases with the decrease of humidity and the increase of temperature (Chow et al., 2008; Takahama et al., 2004). Also, complete evaporation may occur beyond 25°C (Schaap et al., 2004). Chow et al. (2008) observed the evaporation loss from quartz filter to be more

than 80% during the warm season in central California. The high temperature (35°C-48°C) during the long sampling hours (24 hours) may be a possible reason for the poor correlation between online and offline $NO_3^-$ measurements during the summer campaign at IITD. Chow et al., (2008) observed the evaporation loss from quartz filter to be more than 80% during the warm season in central California. A study by Schaap et al., (2004) reported that the $NO_3^-$ volatilization during a 24-h sampling period not only depends on the sampling apparatus instruments and ambient conditions, but also a function of on sampling strategy. If the sampling strategy is evening to evening (24 hours), the samples will lose the $NO_3^-$ sampled during night as evaporation with the increasing temperature during the day. increases during the day with the increase in temperature. However, during morning-to-morning strategy, the filters will collect the $NO_3^-$ quantatively at night, and the higher temperature in the afternoon of the previous day may promote the loss of $NO_3^-$ from the filter (Malaguti et al., 2015). In this study, the sampling time was from 6:30 am to the next day 6.30 am. Therefore, the filter-based inorganic measurements suffered from a negative sampling artifact due to the evaporation of nitrate collected during the forenoon in a temperature of 20°C-25°C during the winter campaign and ~ 38°C-45°C during the summer campaign.

Table 2. Regression coefficients and slopes for the comparison of WSIS measured by HR-ToF-AMS and IC.

| Sites | $NO_3^-$ | | $SO_4^{2-}$ | | $NH_4^+$ | | $Cl^-$ | |
|---|---|---|---|---|---|---|---|---|
| | $R^2$ | Slope | $R^2$ | Slope | $R^2$ | Slope | $R^2$ | Slope |
| **IITD Summer** | 0.42 | 1.78 | 0.93 | 0.17 | 0.91 | 0.49 | 0.55 | 0.33 |
| **IITD Winter** | 0.82 | 0.49 | 0.82 | 0.68 | 0.76 | 0.99 | 0.82 | 0.79 |
| **IITMD Winter** | 0.91 | 1.07 | 0.93 | 0.93 | 0.89 | 0.93 | 0.82 | 0.88 |

We observed higher $Cl^-$ concentration in filter-based measurement than online measurement using HR-ToF-AMS during both campaigns at IITD and winter at IITMD. A good correlation of $R^2= 0.82$ with a slope of 0.79 and $R^2= 0.82$ with a slope of 0.88 was observed during the winter campaign at IITD and IITMD, respectively (Fig. 3). Interestingly, during the summer campaign at IITD the comparability was moderate with a correlation coefficient of $R^2= 0.55$ and a slope of 0.33. A correlation coefficient of $R^2= 0.83$ between Dp <10 μm measured with the MARGA and analyzed from Teflon filters was reported in Makkonen et al., (2012) during Feb-May. Lower temperature and higher RH during winter retains $Cl^-$ in particulate phase for long enough to be detected which is not the case in summer. Further, $Cl^-$ is predominantly found in the coarse fraction. Also, while AMS only measures the NR-$Cl^-$ (Manchanda et al., 2021), e.g. $NH_4Cl$, which can vaporize at 600˚C but cannot measure $Cl^-$ from refractory-KCl, IC measures chloride from all the water-soluble chloride salts, including $NH_4Cl$ and KCl. This probably justifies the lower concentration of $Cl^-$ in online measurement from AMS than filter-based measurements. We also compared $Cl^-$ measurements from

Xact 625i with the measurements from IC. Interestingly, IC measurements of Cl⁻ were also found to be higher than Xact 625i measurements during summer at IITD and winter at IITMD. Interestingly, Tthe Cl⁻ measurements from Xact 625i were ~1.9 times higher than the measurements from IC during winter at IITD (see fig. SM2 in supplementary material). The correlations were found to be good during winter ($R^2$= 0.83 and 0.76 at IITD and IITMD respectively) and worsen during summer ($R^2$= 0.27 at IITD), similar to what we observed for AMS_Cl⁻ and IC_ Cl⁻. Lower temperature and higher RH during winter retains Cl⁻ in particulate phase for long enough to be detected which is not the case in summer. Further, Cl⁻ is predominantly found in the coarse fraction. Also, while AMS only measures the NR-Cl⁻ (Manchanda et al., 2021), e.g. $NH_4Cl$, which can vaporize at 600°C but cannot measure Cl⁻ from refractory-KCl, IC measures chloride from all the water-soluble chloride salts, including $NH_4Cl$ and KCl. It could be due to the differences in water-soluble fraction of chloride in the samples, as ionic concentration (IC) represents water-soluble fraction whereas elemental concentration (Xact 625i) represents total concentration. Also, a lot particulate bound chloride in the atmosphere is in the form of ammonium chloride (Manchanda et al., 2021). Part of the ammonium chloride collected during the day long offline sampling would have vaporized, giving lower concentration from IC measurements. Further investigation is needed to draw a firm conclusion. On the other hand, Xact 625i measures Cl⁻ from both the salts using XRF technique. This probably justifies the lower concentration of Cl⁻ in online measurements than filter-based measurements and better slopes (closer to unity) with Xact than AMS.

**3.2 Online and offline measurements of heavy and trace metals and their comparison**

For the inter-comparison of heavy and trace metal concentrations from Xact 625i and ICP-MS, the half-hourly Xact 625i data were averaged to 24 hours filter sampling interval. A total of 32 elements were analyzed on each filter using ICP-MS while, 27 elements were measured in Xact 625i at IITD during summer and winter campaign, and 30 elements were measured in Xact 625i at IITMD during the winter campaign. The spatial and temporal variations of the crustal and trace elements are shown in Fig. SM3. Al and Ca concentrations were the most abundant in ICP-MS and Xact measurements respectively during the summer season (Fig. 4a, 5a & 5b) because of the increase in the crustal activities whereas K concentrations were significantly high for both the measurements during winter (Fig. 4d, 4g, 5c, 5d, 5e and 5f) due to mass-scale agricultural crop-residue burning in the adjoining states of Punjab and Haryana. Elements emitted from anthropogenic activities, e.g., coal-fired power plants (As, Se, Hg, Pb), traffic emissions (Cr, Pb, Mn), wear debris emission (Cu, Cd, Fe, Ga, Mn, Mo), etc. are found to be in higher concentration during winter campaign than summer campaign for both the measurements. Similar results were observed in our companion paper Shukla et al. (2021). The average values of metals along with their ranges are tabulated

417    in Table SM2 and the statistics involved mean, upper, and lower values of some major elements are shown

418    in Fig. 4. Box plots for rest of the metals can be found in Fig. SM4.

419

420

421

422

423

424

425

426
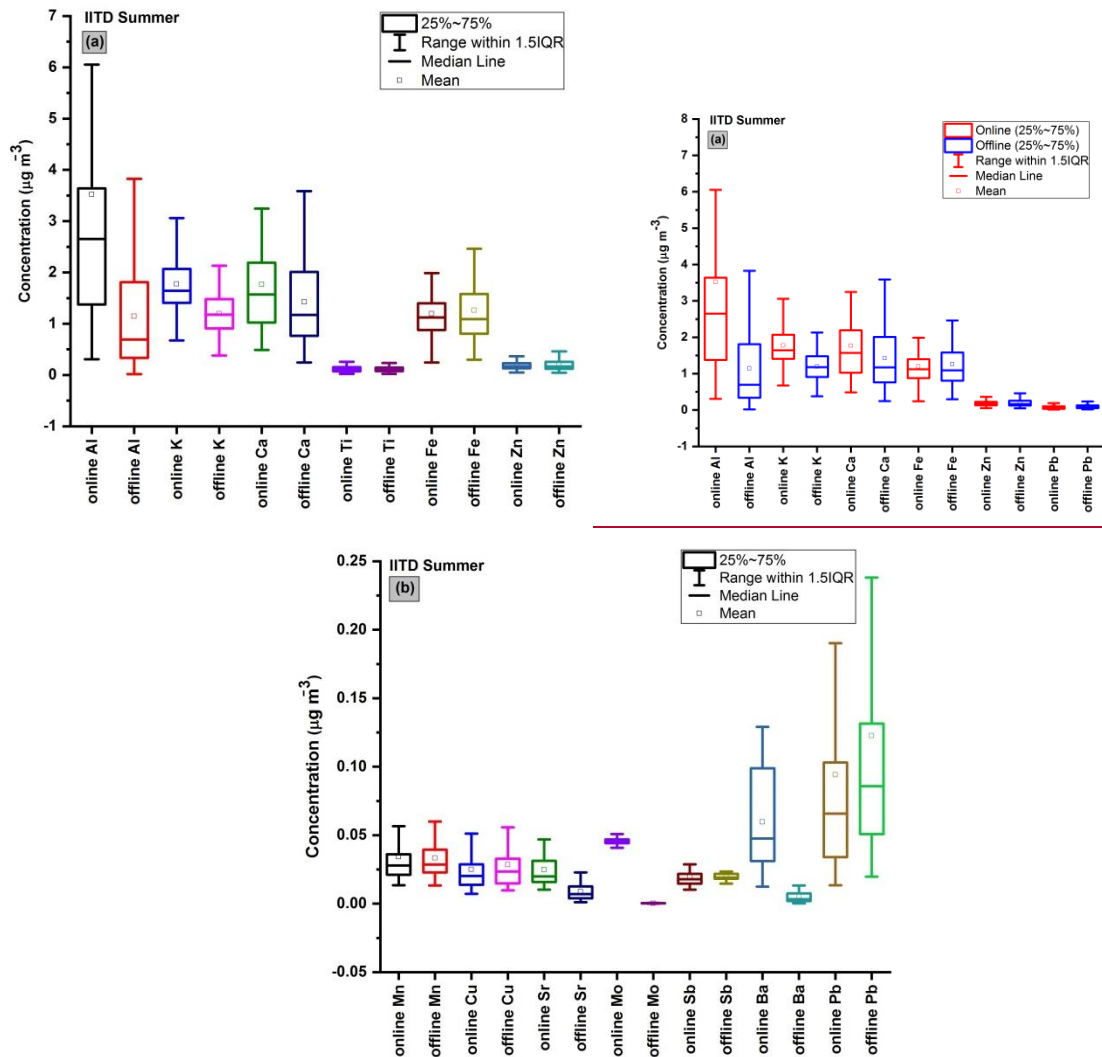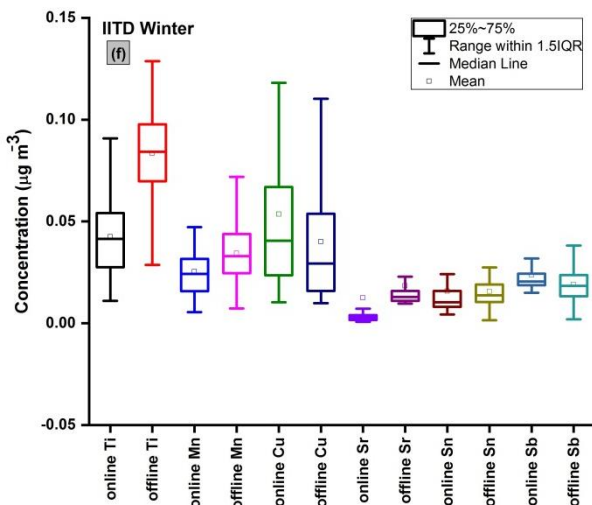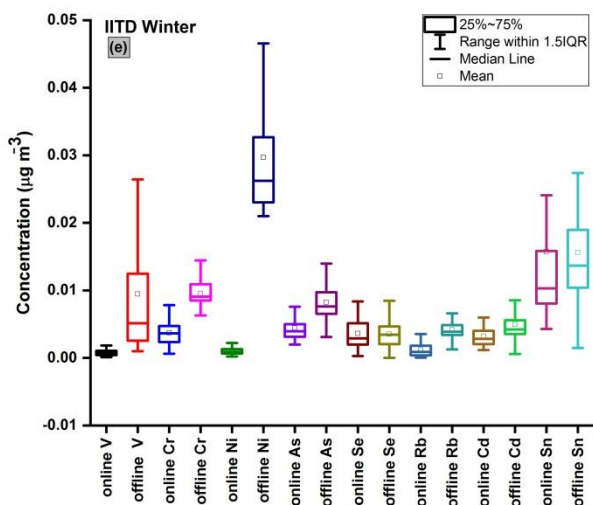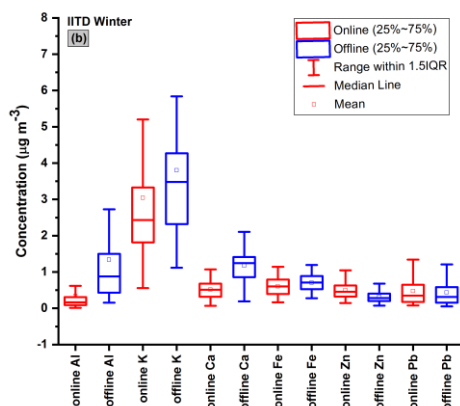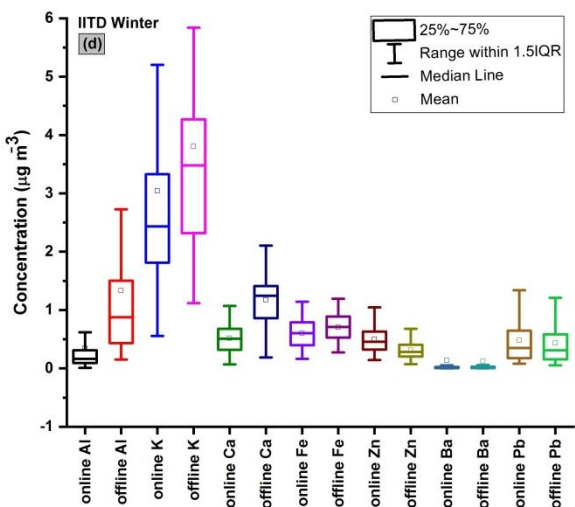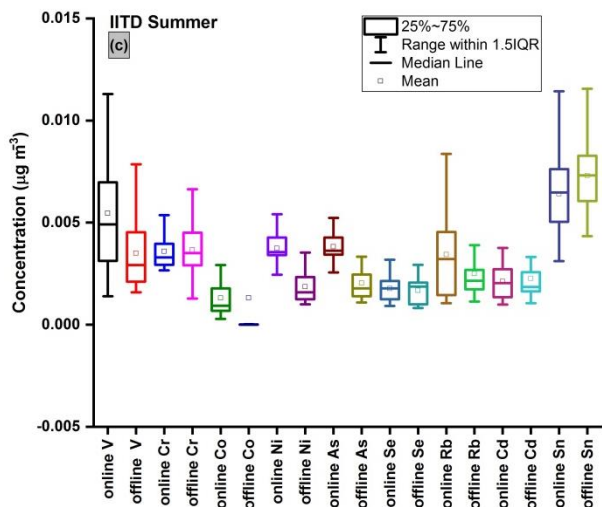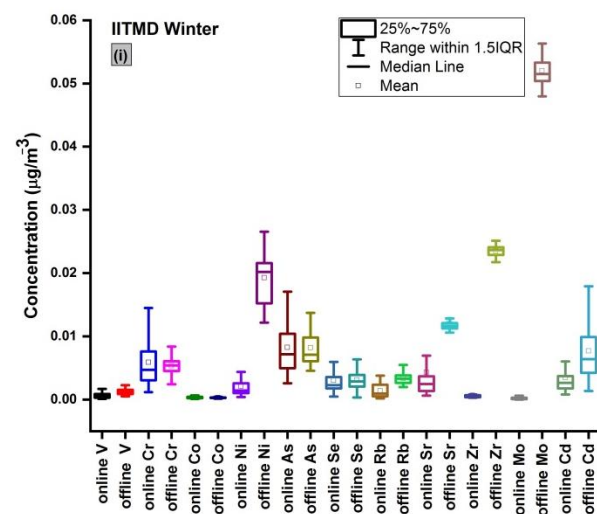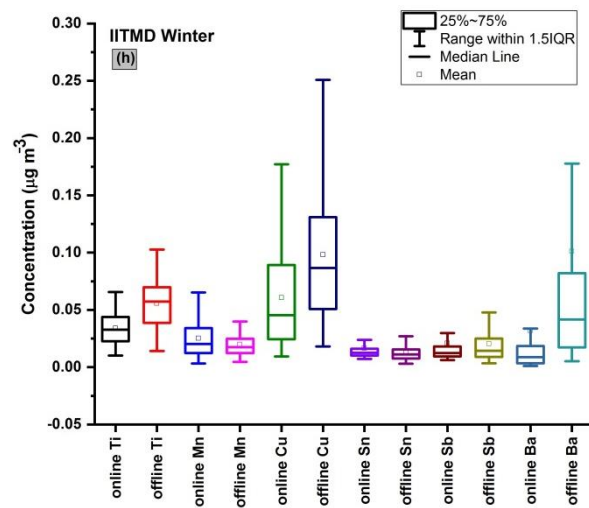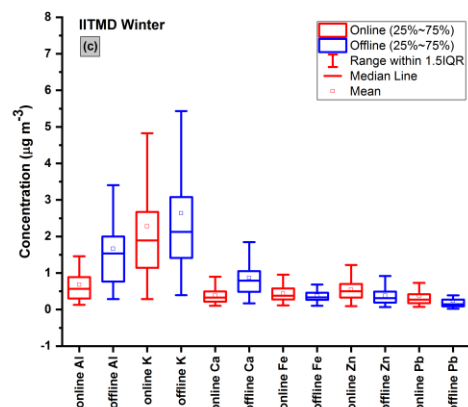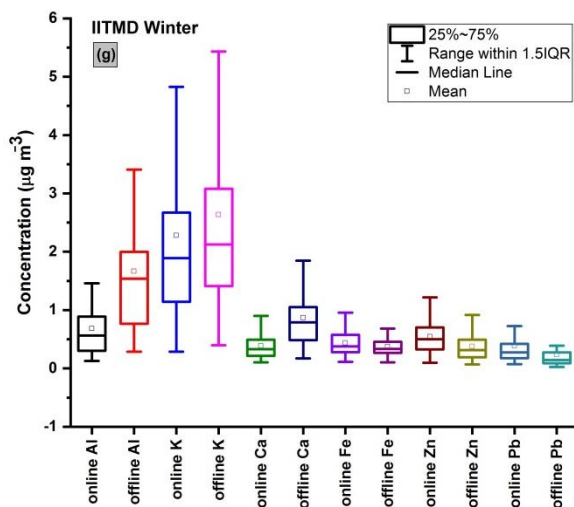
427 Fig.4. Box plots of online and offline measured heavy and trace metals during (a,b,c) summer campaign at

428 IITD, (d,e,f) winter campaign at IITD, and (g,h,i) winter campaign at IITMD site. The box plots for rest of

429 the heavy and trace elements are shown in fig. SM4 of the supplementary material.

430 The trends of the elemental concentration in decreasing order for both ICP-MS and Xact measurements

431 during summer and winter at IITD and winter at IITMD are shown in Fig. SM4. The trace metals such as

432 Cd, Mn, Mo, Ba, Pd etc. contribute a small portion in $PM_{2.5}$ in terms of their mass concentration but have a

433 significant effect on human health. Fractions of elements in total element concentration for both the

434 measurements during summer and winter campaign at IITD and during winter campaign at IITMD were

435 shown in Fig. 5.

436

437
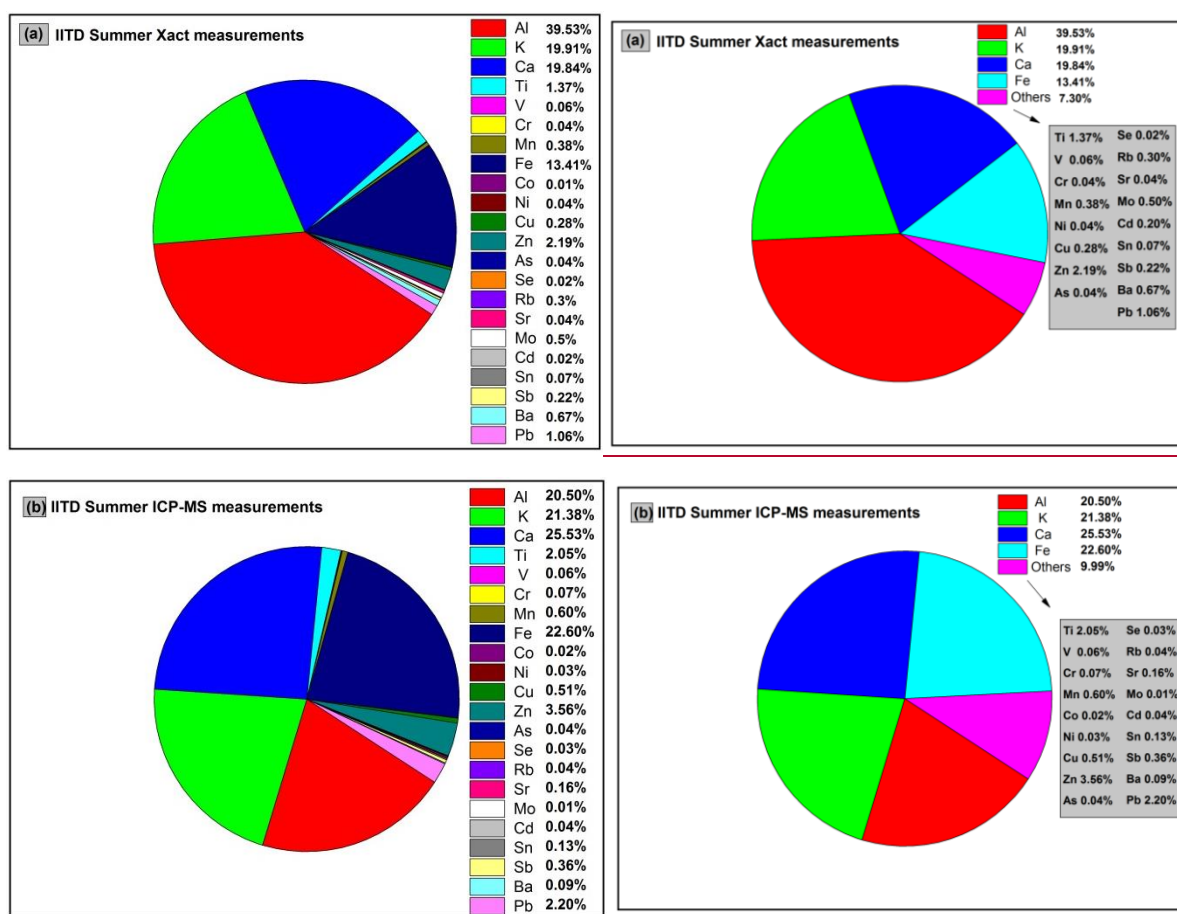
438
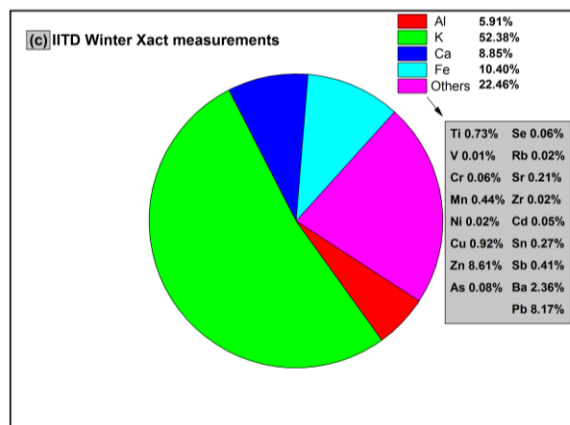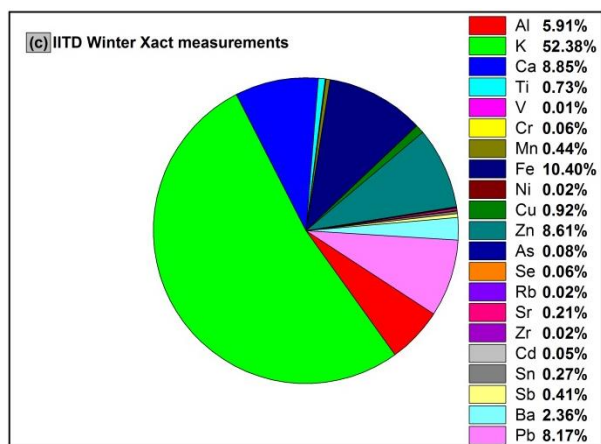
439
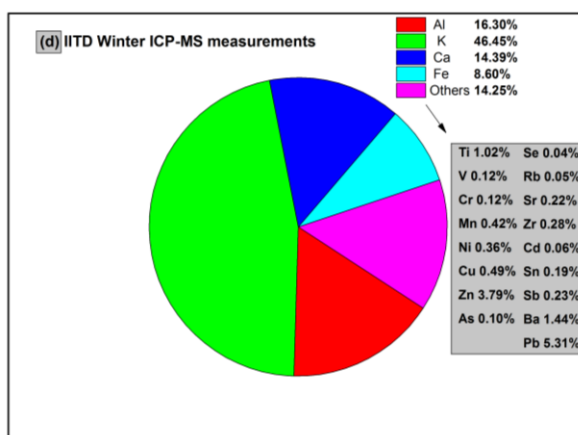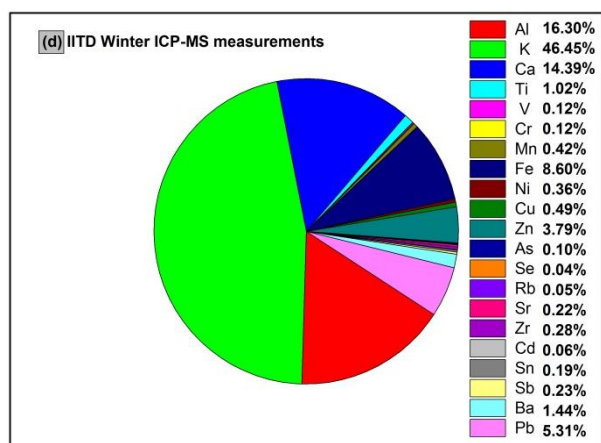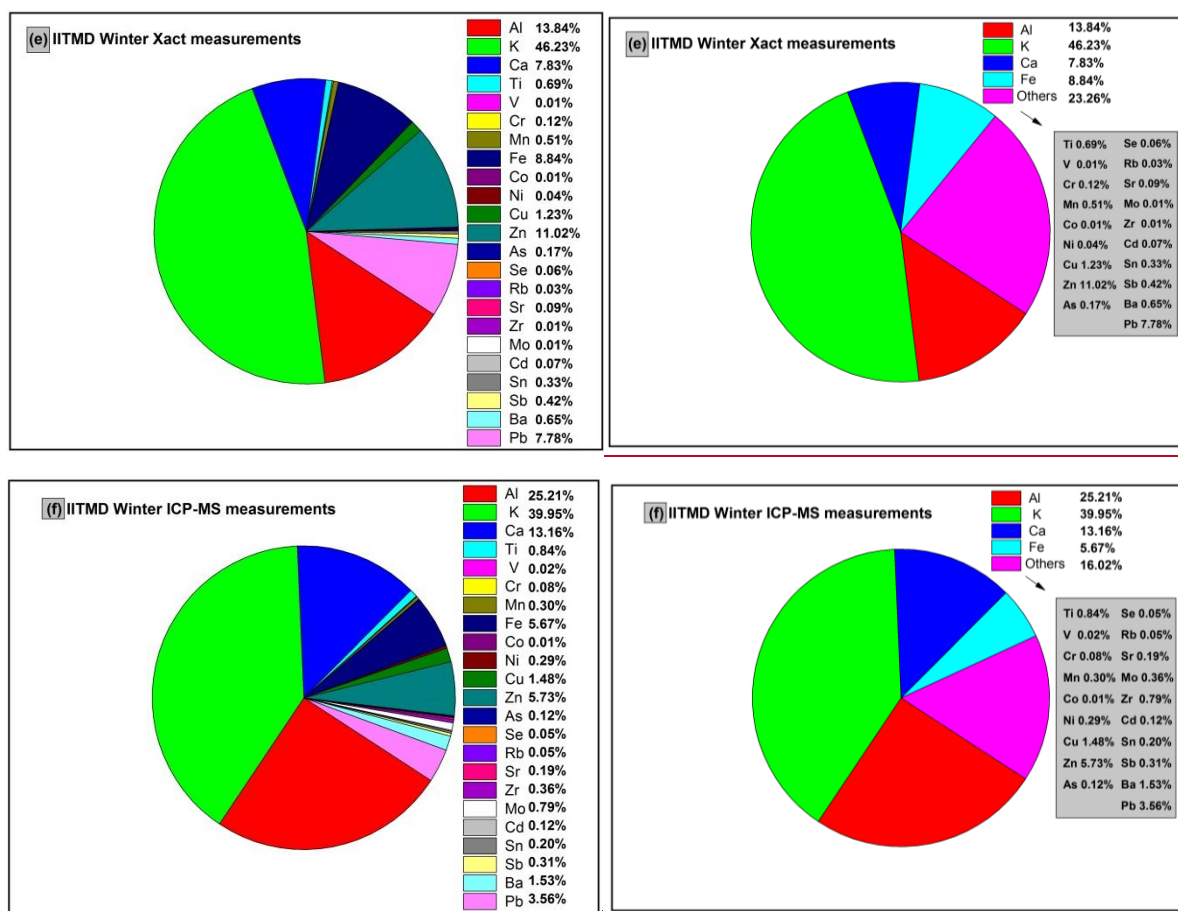
Fig.5. Fractions (%) of elements in total element concentration in PM$_{2.5}$ presented in pie format for online (a,c,e) and offline (b,d,f) measurements during winter and summer at IITD and during winter at IITMD.

MDLs for ICP-MS measurements were calculated according to Escrig Vidal et al., (2009), and MDLs for Xact 625i were obtained from the manufacturer. MDLs for the Xact 625i and ICP-MS are listed in Table SM2 in the supplementary material. Though the half-hourly Xact data were averaged to 24 hours to the corresponding interval of the filter sampling, for comparability check, MDLs of Xact 625i measurements were taken for 30 mins sampling time while MDLs of filter-based elemental measurements were calculated for 24 hours. Elements having data below $3 \times$ MDL were discarded from further examination and unreliable as values below $3 \times$ MDL would lead to higher uncertainty (Furger et al., 2017). The elements K, Ca, Ti, Mn, Fe, Ba, and Pb have >80% of their values above both offline and online MDLs, and thus the data quality is reliable. Further, Ni, Mo, Zr have higher blank concentrations, and thus the data is not reliable for ICP-MS measurements. Data below $3 \times$ MDL value were discarded from the data set as it would lead to higher uncertainty (Furger et al., 2017). The elements K, Ca, Ti, Mn, Fe, Ba, and Pb have >80% of their values above both offline and online MDLs, and thus the data quality is reliable. Further, Ni, Mo, Zr have

456 ~~higher blank concentrations, and thus the data is not reliable for ICP-MS measurements.~~ The comparability

457 of the elements measured online using Xact 625i with those analysed using an ICP-MS, was checked for

458 the common elements in these two measurements (21 elements for IITD and 23 elements for IITMD) and

459 is shown in Fig. 6.

460

461

462

463

464

465

466

467
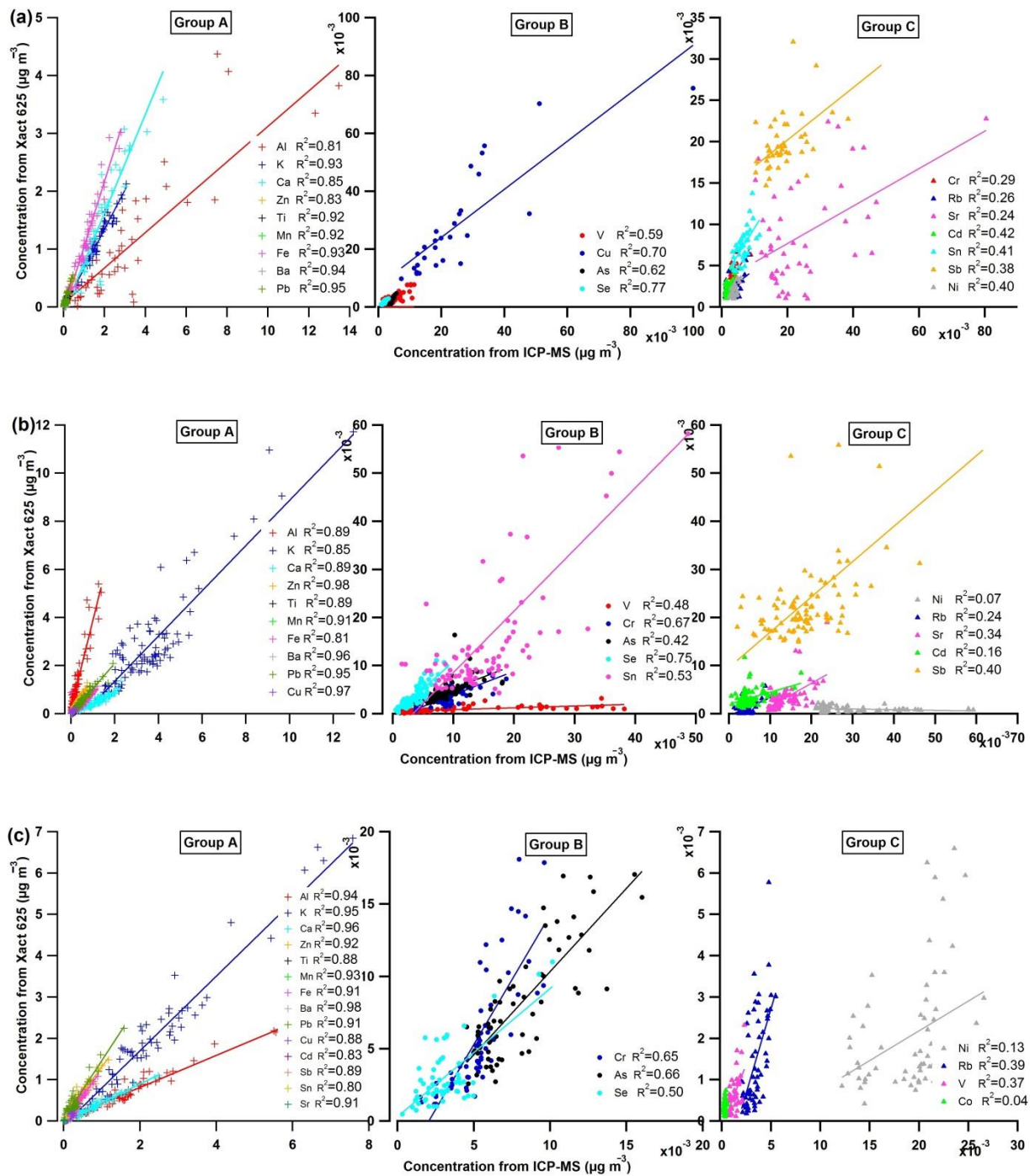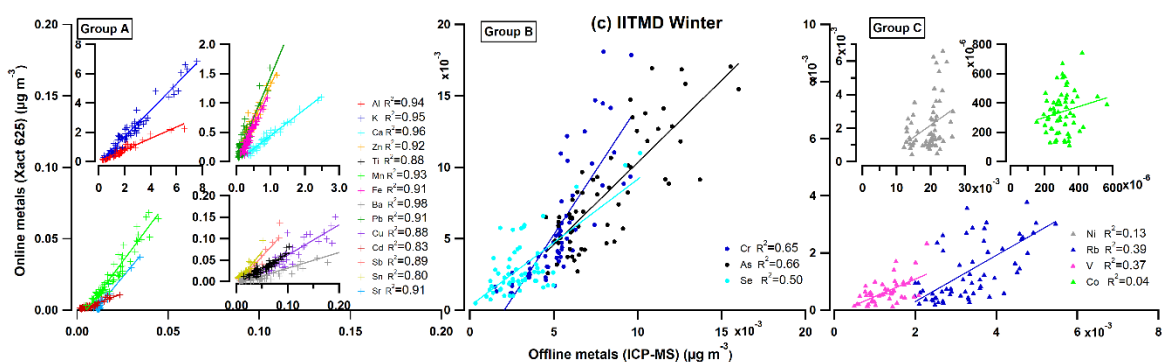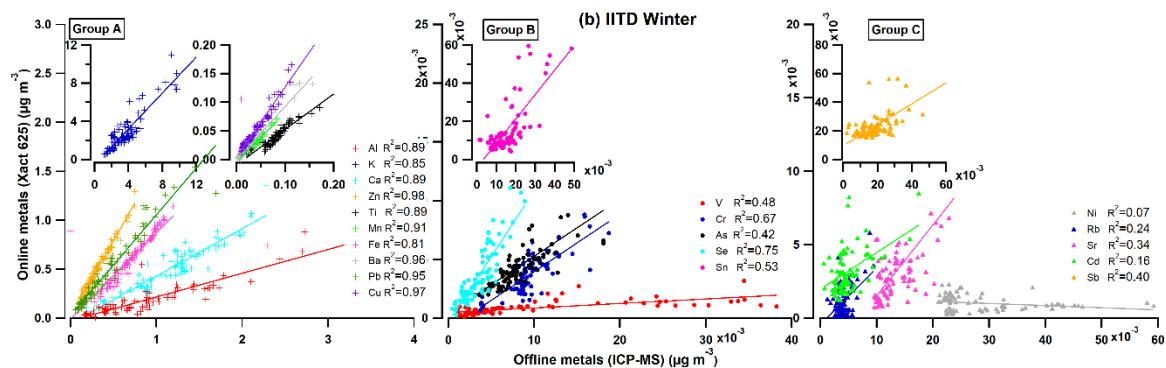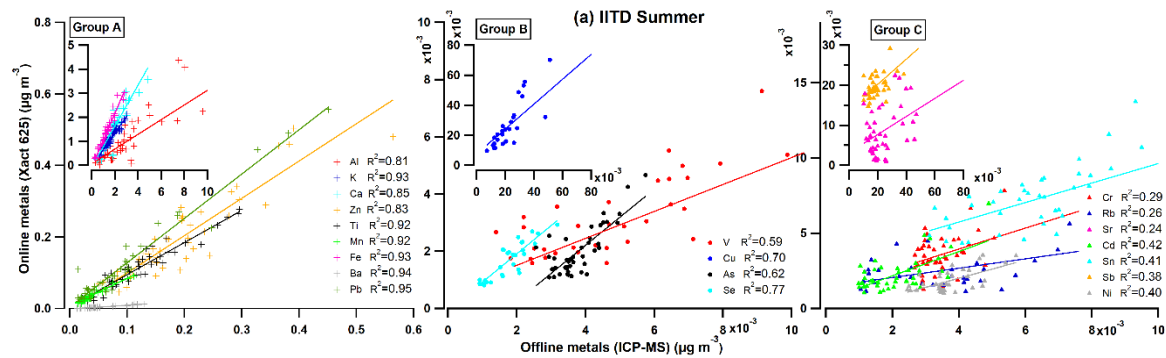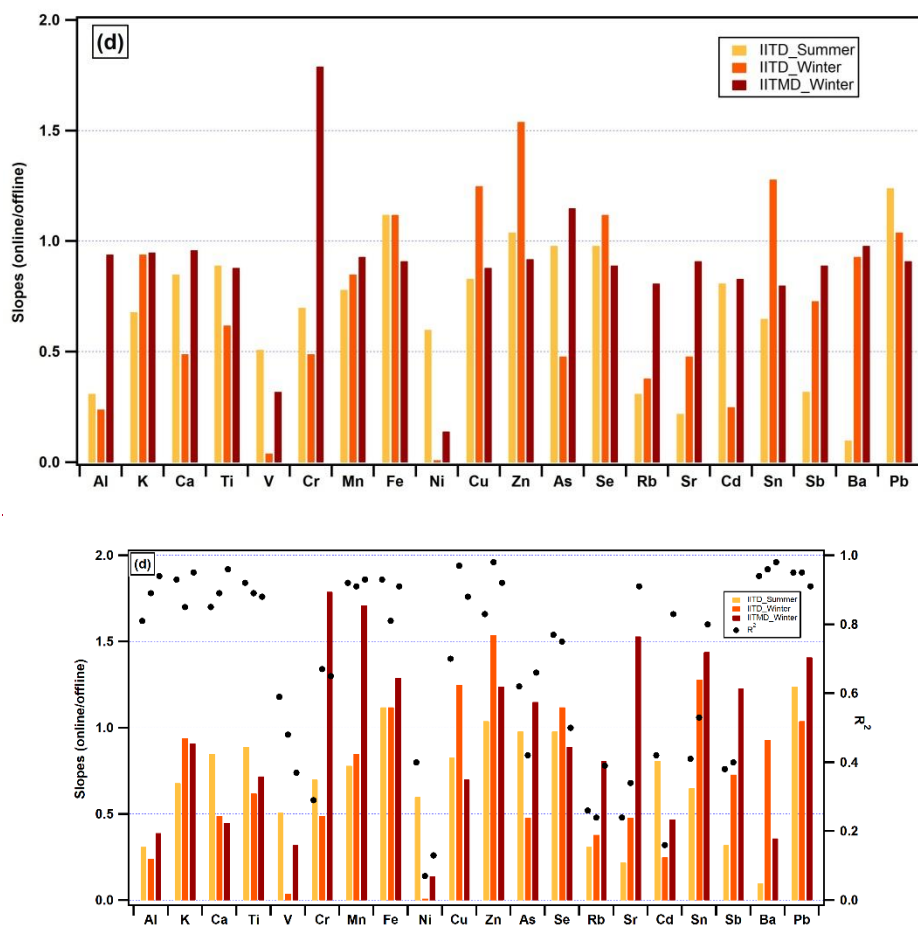
Fig. 6. Scatter plots and regression lines of Xact 625i vs. ICP-MS data for groups A, B, and C during (a) summer at IITD, (b) winter at IITD, (c) winter at IITMD, and (d) comparison of slopes (online/offline) & $R^2$ of the measured heavy and trace metals in $PM_{2.5}$ during the summer and winter campaign at IITD and winter campaign at IIITMD.

Based on their comparability characteristics, elements were grouped under 3 categories. Group A showed excellent linearity between the two methods with a correlation coefficient of $R^2 > 0.8$. Overall, group A consists of Al, K, Ca, Ti, Mn, Fe, Cu, Zn, Ba, and Pb during winter at IITD whereas, Cu showed in another group during summer at IITD. Though Sr, Cd, Sn, Sb had average values below MDLs and posed a lower correlation coefficient at IITD, interestingly, Sr, Cd, Sn, and Sb joined group A during winter at IITMD. To distinguish the potential difference in accuracy between the two methods, intercepts were not forced to be zero. The slopes are important, which indicate biases between the two measurements. The slopes of Zn, Fe, and Pb were closer to unity during summer at IITD (Fig. 6). K, Fe, Cu, Zn, Ba, and Pb achieved a slope of 0.94-1.25 during winter at IITD whereas, Mn, Fe, Zn, Pb, Sr, Sn, and Sb pose a slope slightly higher than unity during winter at IITMD (Fig. 6). A slight difference in cut-off value for the particle size can

482    reduce the slopes from unity and produce ~10% difference in collected mass (Panteliadis et al., 2012). The

483    slopes and the correlation coefficients are listed in Table 3.

484    In a comparison study conducted by USEPA & Etv. (2012) between Xact 625i and ICP-MS measurements,

485    Ca, Cu, Mn, Pb, Se, and Zn were highly correlated except Cu. Cu was close to the MDL values of ICP-MS

486    and Xact 625i. A good agreement was observed between Xact 625i and offline measurements using ED-

487    XRF in South Korea by Park et al., (2014). The comparability between Xact measurements and ICP-MS

488    measurements was checked for the elements As, Ba, Ca, Cr, Cu, Fe, K, Mn, Ni, Pb, Se, Sr, Ti, V, and Zn

489    in Tremper et al. (2018). They observed an average $R^2$ of 0.93 and a slope of 1.07 for these elements. In the

490    study by Furger et al., (2017) during a warmer season in Switzerland, an excellent correlation ($R^2$>0.95)

491    was found for Xact and ICP-OES/MS measurements of S, K, Ca, Ti, Mn, Fe, Cu, Zn, Ba, and Pb. However,

492    they found that the elemental measurements by Xact 625i were 28% higher than ICP-OES/MS

493    measurements for these 10 elements. In our study, Xact measurements of Fe, Cu, Zn, and Pb yielded an

494    average of 24% higher mass concentrations than ICP-MS measurements for Group A elements during

495    winter at IITD. Xact measurements were systematically 10% (average) higher than ICP for Zn, Fe, and Pb

496    during summer at IITD, whereas;  we obtained an average of 41% higher Xact measurements than ICP for

497    Mn, Fe, Zn, Pb, Sr, Sn, and Sb during winter at IITMD in Group A elements.

498    Group B was characterized by moderate linearity having $R^2$~0.4-0.8 and consisted of the elements V, Cu,

499    As, and Se during summer at IITD; V, Cr, As, Se, Sn during winter at IITD and Cr, As and Se during winter

500    at IITMD. These elements in Group B had their values very close to or below  MDLs of at least one of the

501    analysis methods. During winter at both sites, Cr and As from ICP-MS have ~50-65% of their values below

502    MDLs, whereas ~68-72% of their values were above the MDLs of Xact 625i. Though some of the elements

503    in this group in different seasons have slopes near or greater than unity (see Table 3) like Group A, their

504    comparison is not statistically feasible.

505    Table 3. Regression coefficients and slopes for the comparison of Xact 625i and ICP-MS measurements.

| Sites | Group A | Slope | $R^2$ | Group B | Slope | $R^2$ | Group C | Slope | $R^2$ |
|-------|---------|-------|-------|---------|-------|-------|---------|-------|-------|
| | Al | 0.31 | 0.81 | V | 0.51 | 0.59 | Cr | 0.7 | 0.29 |
| | K | 0.68 | 0.93 | Cu | 0.83 | 0.70 | Co | - | - |
| | Ca | 0.85 | 0.85 | As | 0.98 | 0.62 | Rb | 0.31 | 0.26 |
| **IITD Summer** | Zn | 1.04 | 0.83 | Se | 0.98 | 0.77 | Sr | 0.22 | 0.24 |
| | Ba | 0.1 | 0.94 | | | | Mo | - | - |
| | Ti | 0.89 | 0.92 | | | | Cd | 0.81 | 0.42 |

| Site | El | | | El | | | El | | |
|---|---|---|---|---|---|---|---|---|---|
| | Mn | 0.78 | 0.92 | | | | Sn | 0.65 | 0.41 |
| | Fe | 1.12 | 0.93 | | | | Sb | 0.32 | 0.38 |
| | Pb | 1.24 | 0.95 | | | | Ni | 0.6 | 0.4 |
| **IITD Winter** | Al | 0.24 | 0.89 | V | 0.04 | 0.48 | Ni | 0.01 | 0.07 |
| | K | 0.94 | 0.85 | Cr | 0.49 | 0.67 | Rb | 0.38 | 0.24 |
| | Ca | 0.49 | 0.89 | As | 0.48 | 0.42 | Sr | 0.48 | 0.34 |
| | Ti | 0.62 | 0.89 | Se | 1.12 | 0.75 | Zr | - | - |
| | Mn | 0.85 | 0.91 | Sn | 1.28 | 0.53 | Cd | 0.25 | 0.16 |
| | Fe | 1.12 | 0.81 | | | | Sb | 0.73 | 0.40 |
| | Cu | 1.25 | 0.97 | | | | | | |
| | Zn | 1.54 | 0.98 | | | | | | |
| | Ba | 0.93 | 0.96 | | | | | | |
| | Pb | 1.04 | 0.95 | | | | | | |
| **IITMD Winter** | Al | 0.39 | 0.94 | Cr | 1.79 | 0.65 | Ni | 0.14 | 0.13 |
| | K | 0.91 | 0.95 | As | 1.15 | 0.66 | Rb | 0.81 | 0.39 |
| | Ca | 0.45 | 0.96 | Se | 0.89 | 0.5 | Mo | - | - |
| | Ti | 0.72 | 0.88 | | | | Zr | - | - |
| | Mn | 1.71 | 0.93 | | | | V | 0.32 | 0.37 |
| | Fe | 1.29 | 0.91 | | | | Co | 0.36 | 0.04 |
| | Cu | 0.70 | 0.88 | | | | | | |
| | Zn | 1.24 | 0.92 | | | | | | |
| | Ba | 0.36 | 0.98 | | | | | | |
| | Pb | 1.41 | 0.91 | | | | | | |
| | Sr | 1.53 | 0.91 | | | | | | |
| | Cd | 0.47 | 0.83 | | | | | | |
| | Sn | 1.44 | 0.8 | | | | | | |
| | Sb | 1.23 | 0.89 | | | | | | |

506     The Group C elements, e.g., Ni, Rb, Sr, Zr, Cd, and Sb during summer at IITD; Cr, Co, Rb, Sr, Mo, Cd,
507     Sn, Sb, and Ni during winter at IITD and, Ni, Rb, Mo, Zr, V, and Co during winter at IITMD are
508     characterized by their bad correlation ($R^2<0.4$). Interestingly, measurements of some element e.g. Mo
509     during summer and winter at IITD and IITMD respectively, Co during summer at IITD, and Zr during
510     winter at both sites from both the methods did not correlate at all. For most of the elements in this group,

511  70-85% of measurements were below both method's MDLs and rest of the data were below $3 \times$ MDLs.
512  The high and variable blank concentrations of these elements increased the MDL values in ICP-MS
513  measurement. The particle size dependent self-absorption effect and line interference between different
514  elements in Xact measurement could also increase the MDL values (Furger et al., 2017). This is probably
515  the reason for the values lower than MDLs for the elements in this group.

516  Overall, we observed 10-40% higher Xact measurements than ICP for some of the elements in Group A
517  during different seasons. The difference in the Xact and High-volume sampler inlet location and their
518  distance from the road can cause such difference in measurements (Furger et al., 2017). In the case of dust
519  resuspension from vehicular traffic, the number concentration of finer particulate matter tends to decrease
520  sharply within an increment of just 50m from the roadway (Hagler et al., 2009). In this study, we tried to
521  co-locate the two sample inlets, but it could not be avoided. Also, IITD and IITMD are both very close
522  (<200 m) to a roadway with moderate to heavy-duty traffic. The differences in online and offline
523  measurements may indicate a gradient in some elements due to very close proximity to heavy-duty traffic.
524  Also, the different temperatures of the sample inlets may give rise to a difference in measured
525  concentrations from both methods (Tremper et al., 2018). In this study, the blank corrected ICP-MS
526  measurements may result in overestimation or underestimation due to variable and high blank
527  concentration. The difference can also occur due to the digestion recovery rate for the digestion protocol
528  used for the filter analysis. Moreover, if the ambient elemental concentration is much lower than the
529  standards used for calibration of Xact, such differences may occur (Indresand et al., 2013).

530  **4. Conclusion**

531  Atmospheric WSIS ($NO_3^-$, $SO_4^{2-}$, $NH_4^+$, $Cl^-$) and heavy and trace elements in $PM_{2.5}$ were measured using
532  offline methods (IC for WSIS and ICP-MS for elements) and online methods (HR-ToF-AMS for inorganics
533  and Xact 625i for elements). These measurements were compared to assess the measurement quality and
534  sampling artifacts of these measurement techniques in the heavily polluted Delhi-NCR for two different
535  metrological conditions (winter and summer season). Field campaigns were conducted at two NCR sites,
536  namely, IITD during June-July 2019 and Oct-Dec 2019 and at IITMD during Oct-Dec 2019. The key
537  findings of this study are summarized below.

538  - $NH_4^+$ concentrations from the IC and HR-ToF-AMS, compared well during winter with a slope of
539    0.99 at IITD and 0.93 at IITMD. Interestingly, $NH_4^+$ concentrations were higher in offline
540    measurements during summer at IITD. The decrease in slope was probably due to the formation
541    of particulate $(NH_4)_2SO_4$.

- Offline $SO_4^{2-}$ measurements were higher (with a slope of 0.17 during summer at IITD and 0.8 and 0.93 during winter at IITD and IITMD, respectively) during both seasons at both the sites due to the positive sampling artifact. The absorption of $SO_2$ and the oxidation or condensation process may result in additional sulphate.

- Lower $NO_3^-$ concentrations (with a slope of 1.78 during summer at IITD and 1.07 during winter at IITMD) were observed in the offline measurement during summer at IITD and during winter at IITMD because of the evaporation of $NH_4NO_3$ from the filter substrates. The evaporative loss of nitrate from the filters was minimal in winter at IITMD. It aggravated during summer at IITD due to the evaporation of ammonium nitrate in such a high temperature (35˚C-48˚C) range. The higher $NO_3^-$ concentrations (slope~0.49) in the filters than HR-ToF-AMS measurements during winter at IITD can be due to the absorption of gas-phase $HNO_3$ on the filter.

- Offline $Cl^-$ was consistently higher (with a slope of 0.33 during summer at IITD and 0.79 and 0.88 during winter at IITD and IITMD, respectively) than HR-ToF-AMS measurements during both seasons at both sites mainly because HR-ToF-AMS only measures the NR-$Cl^-$ whereas, the offline $Cl^-$ measurements includes chloride from all the water-soluble chloride salts. The comparability degrades during summer due to the volatile nature of $Cl^-$ in higher temperatures and lower RH.

- The elements were grouped into three categories (Group A, B and C) according to their comparability characteristics. The elemental data from Xact 625i were highly correlated ($R^2$>0.8) with ICP-MS measurements of the 24 hr filters for Group A elements (Al, K, Ca, Ti, Zn, Mn, Fe, Ba, and Pb). The Cu also showed up in this group during winter at IITD. About 80% of the data for these elements were above MDLs for both the methods. Though Sn, Sb, and Cd had values below MDLs of one or both the methods, interestingly, they were highly correlated ($R^2$>0.8) and, slopes are very close to unity for Sn and Sb during winter at IITMD. The correlation coefficients > 0.8 for the elements in Group A indicated the high precision of the online and offline measurements. Hence, these elements from any of these methods can be reliably used for modelling studies.

- The elements under Group B had their values closer to or below at least one of the method's MDLs. Cr and As had ~50-65% of their values below ICP-MS MDLs from ICP-MS, whereas ~68-72% of their values were above Xact 625i MDLs during winter at both sites.

- Elements like Ni, Mo, and Zr measured from ICP-MS were not reliable due to their higher and variable blank concentrations. No conclusion on their measurement accuracy by the two methods can be drawn.

- In summary, the daily averaged half-hourly Xact 625i measurements were 10-40% higher than 24 hr filter measurements by ICP-MS depending upon the seasons, sites and elements in Group A.

576        Distance between two inlets for the two methods, distance of the inlets from the roadway, line

577        interference between two elements in Xact measurements, particle size, sampling strategy, filter

578        type, higher and variable concentrations in blank filters and digestion protocol for ICP

579        measurements can cause the difference in measurements between the two methods.

580 ~~The above findings highlight the measurement methods' accuracy and implement the particular type of~~

581 ~~measurements as needed. Future work should involve using different filter substrates and different digestion~~

582 ~~protocols to reevaluate the difference between these online and offline methods. Although this study~~

583 ~~compares the PM species, a comparison of full source apportionment analysis between online and offline~~

584 ~~methods should be done for more qualitative and quantitative insights.~~ The above findings highlight the

585 measurement methods' accuracy and implement the particular type of measurements as needed. Denuders

586 could be effective in avoiding the overestimation problems of ammonium and sulphate in filter

587 measurements and improve the comparison. Also, teflon filters instead of quartz filters in the un-denuded

588 sampler are reported to give better comparison for sulphate. The MDLs in the Xact 625 measurements are

589 higher than the MDLs for the offline method. Depending on the objective of the campaign, Xact 625 can

590 be deployed for a longer time interval to analyse the elements that are below their MDLs. The high

591 resolution real-time monitoring of non-refractory organics, inorganics by HR-ToF-AMS and elements by

592 Xact comes at the cost of high sensitivity in MDLs, calibrations and cost. Whereas, cost effectiveness of

593 conventional samplers makes it practical to deploy in larger numbers at multi-sites simultaneously. Overall,

594 high resolution real time sampling provides a rich dataset for high and small pollution episodes. Future

595 work should involve using different filter substrates and different digestion protocols to re-evaluate the

596 difference between these online and offline methods. Although this study compares the PM species, a

597 comparison of full source apportionment analysis between online and offline methods should be done for

598 more qualitative and quantitative insights.

599

600 **Author contribution**

601 HSB performed the offline analysis, data processing and wrote the manuscript. JD collected the AMS data

602 at IITD. AS and VL carried out the Xact and AMS data collection and processing respectively. NR, MK,

603 VS and SNT were involved with the supervision and conceptualization. All co-authors contributed to the

604 paper discussion and revision.

605 **Declaration of interests**

606     The authors declare that they have no conflict of interest.

607     **Acknowledgements**

608     The authors are thankful to Naba Hazarika and Mohd Faisal for collecting the Xact data at IITMD and
609     Pawan Vats for the sampling and collection of the filters at IITD. The authors are also thankful to Amit
610     Vishwakarma, Vaibhav Shrivastava and Harishankar for helping in offline analysis. This work is financially
611     supported by the Department of Biotechnology, Government of India (Grant No.
612     BT/IN/UK/APHH/41/KB/2016-17 dated 19th July 2017) and Central Pollution Control Board (CPCB),
613     Government of India to conduct this research under grant no. AQM/Source apportionment_EPC
614     Project/2017 dated 12th February 2019.

615     **Reference**

616     Bhowmik, H. S., Naresh, S., Bhattu, D., Rastogi, N., Prévôt, A. S. H., & Tripathi, S. N. (2020). Temporal
617         and spatial variability of carbonaceous species (EC; OC; WSOC and SOA) in PM2.5 aerosol over
618         five sites of Indo-Gangetic Plain. *Atmospheric Pollution Research*, *12*(June 2020), 375–390.
619         https://doi.org/10.1016/j.apr.2020.09.019

620     Chen, Y., Xu, L., Humphry, T., Hettiyadura, A. P. S., Ovadnevaite, J., Huang, S., Poulain, L., Schroder, J.
621         C., Campuzano-Jost, P., Jimenez, J. L., Herrmann, H., O'Dowd, C., Stone, E. A., & Ng, N. L.
622         (2019). Response of the Aerodyne Aerosol Mass Spectrometer to Inorganic Sulfates and
623         Organosulfur Compounds: Applications in Field and Laboratory Measurements. *Environmental*
624         *Science and Technology*, *53*(9), 5176–5186. https://doi.org/10.1021/acs.est.9b00884

625     Chow, J. C. (1995). Measurement methods to determine compliance with ambient air quality standards
626         for suspended particles. *Journal of the Air and Waste Management Association*, *45*(5), 320–382.
627         https://doi.org/10.1080/10473289.1995.10467369

628     Chow, J. C., Watson, J. G., Lowenthal, D. H., Park, K., Doraiswamy, P., Bowers, K., & Bode, R. (2008).
629         Continuous and filter-based measurements of PM2.5 nitrate and sulfate at the Fresno Supersite.
630         *Environmental Monitoring and Assessment*, *144*(1–3), 179–189. https://doi.org/10.1007/s10661-
631         007-9987-5

632     Day, D., Campuzano-Jost, P., Nault, B., Palm, B., Hu, W., Guo, H., Wooldridge, P., Cohen, R., Docherty,
633         K., Huffman, J. A., de Sá, S., Martin, S., & Jimenez, J. (2021). A Systematic Re-evaluation of
634         Methods for Quantification of Bulk Particle-phase Organic Nitrates Using Real-time Aerosol Mass

635        Spectrometry. *Atmospheric Measurement Techniques Discussions*, *2*(3), 1–35.

636        https://doi.org/10.5194/amt-2021-263

637  DeCarlo, P. F., Kimmel, J. R., Trimborn, A., Northway, M. J., Jayne, J. T., Aiken, A. C., Gonin, M.,

638        Fuhrer, K., Horvath, T., Docherty, K. S., Worsnop, D. R., & Jimenez, J. L. (2006). Field-deployable,

639        high-resolution, time-of-flight aerosol mass spectrometer. *Analytical Chemistry*, *78*(24), 8281–8289.

640        https://doi.org/10.1021/ac061249n

641  Escrig Vidal, A., Monfort, E., Celades, I., Querol, X., Amato, F., Minguillón, M. C., & Hopke, P. K.

642        (2009). Application of optimally scaled target factor analysis for assessing source contribution of

643        ambient PM10. *Journal of the Air and Waste Management Association*, *59*(11), 1296–1307.

644        https://doi.org/10.3155/1047-3289.59.11.1296

645  Farmer, D. K., Matsunaga, A., Docherty, K. S., Surratt, J. D., Seinfeld, J. H., Ziemann, P. J., & Jimenez,

646        J. L. (2010). Response of an aerosol mass spectrometer to organonitrates and organosulfates and

647        implications for atmospheric chemistry. *Proceedings of the National Academy of Sciences of the*

648        *United States of America*, *107*(15), 6670–6675. https://doi.org/10.1073/pnas.0912340107

649  Furger, M., Minguillón, M. C., Yadav, V., Slowik, J. G., Hüglin, C., Fröhlich, R., Petterson, K.,

650        Baltensperger, U., & Prévôt, A. S. H. (2017). Elemental composition of ambient aerosols measured

651        with high temporal resolution using an online XRF spectrometer. *Atmospheric Measurement*

652        *Techniques*, *10*(6), 2061–2076. https://doi.org/10.5194/amt-10-2061-2017

653  Gani, S., Bhandari, S., Seraj, S., Wang, D. S., Patel, K., Soni, P., Arub, Z., Habib, G., Hildebrandt Ruiz,

654        L., & Apte, J. S. (2019). Submicron aerosol composition in the world's most polluted megacity: The

655        Delhi Aerosol Supersite study. *Atmospheric Chemistry and Physics*, *19*(10), 6843–6859.

656        https://doi.org/10.5194/acp-19-6843-2019

657  Hagler, G. S. W., Baldauf, R. W., Thoma, E. D., Long, T. R., Snow, R. F., Kinsey, J. S., Oudejans, L., &

658        Gullett, B. K. (2009). Ultrafine particles near a major roadway in Raleigh, North Carolina:

659        Downwind attenuation and correlation with traffic-related pollutants. *Atmospheric Environment*,

660        *43*(6), 1229–1234. https://doi.org/10.1016/j.atmosenv.2008.11.024

661  Hong, C., Zhang, Q., Zhang, Y., Davis, S. J., Tong, D., Zheng, Y., Liu, Z., Guan, D., He, K., &

662        Schellnhuber, H. J. (2019). Impacts of climate change on future air quality and human health in

663        China. *Proceedings of the National Academy of Sciences of the United States of America*, *116*(35),

664        17193–17200. https://doi.org/10.1073/pnas.1812881116

665 Hu, W., Campuzano-Jost, P., Day, D. A., Croteau, P., Canagaratna, M. R., Jayne, J. T., Worsnop, D. R.,

666         & Jimenez, J. L. (2017). Evaluation of the new capture vaporizer for aerosol mass spectrometers

667         (AMS) through field studies of inorganic species. *Aerosol Science and Technology*, *51*(6), 735–754.

668         https://doi.org/10.1080/02786826.2017.1296104

669 Indresand, H., White, W. H., Trzepla, K., & Dillner, A. M. (2013). Preparation of sulfur reference

670         materials that reproduce atmospheric particulate matter sample characteristics for XRF calibration.

671         *X-Ray Spectrometry*, *42*(5), 359–367. https://doi.org/10.1002/xrs.2456

672 Jayne, J. T., Leard, D. C., Zhang, X., Davidovits, P., Smith, K. A., Kolb, C. E., & Worsnop, D. R. (2000).

673         Development of an aerosol mass spectrometer for size and composition analysis of submicron

674         particles. In *Aerosol Science and Technology* (Vol. 33, Issues 1–2, pp. 49–70).

675         https://doi.org/10.1080/027868200410840

676 Jimenez, J. L., Jayne, J. T., Shi, Q., Kolb, C. E., Worsnop, D. R., Yourshaw, I., Seinfeld, J. H., Flagan, R.

677         C., Zhang, X., Smith, K. A., Morris, J. W., & Davidovits, P. (2003). Ambient aerosol sampling

678         using the Aerodyne aerosol mass spectrometer. *Journal of Geophysical Research: Atmospheres*,

679         *108*(7). https://doi.org/10.1029/2001jd001213

680 Lalchandani, V., Srivastava, D., Dave, J., Mishra, S., Tripathi, N., Shukla, A. K., Sahu, R., Thamban, N.

681         M., Gaddamidi, S., Dixit, K., Ganguly, D., Tiwari, S., Srivastava, A. K., Sahu, L., Rastogi, N.,

682         Gargava, P., & Tripathi, S. N. (2022). Effect of Biomass Burning on PM2.5 Composition and

683         Secondary Aerosol Formation During Post-Monsoon and Winter Haze Episodes in Delhi. *Journal of*

684         *Geophysical Research: Atmospheres*, *127*(1), 1–21. https://doi.org/10.1029/2021JD035232

685 Lalchandani, Vipul, Kumar, V., Tobler, A., M. Thamban, N., Mishra, S., Slowik, J. G., Bhattu, D., Rai,

686         P., Satish, R., Ganguly, D., Tiwari, S., Rastogi, N., Tiwari, S., Močnik, G., Prévôt, A. S. H., &

687         Tripathi, S. N. (2021). Real-time characterization and source apportionment of fine particulate

688         matter in the Delhi megacity area during late winter. *Science of the Total Environment*, *770*.

689         https://doi.org/10.1016/j.scitotenv.2021.145324

690 Lipfert, F. W. (1994). Filter artifacts associated with particulate measurements: Recent evidence and

691         effects on statistical relationships. *Atmospheric Environment*, *28*(20), 3233–3249.

692         https://doi.org/10.1016/1352-2310(94)00167-J

693 Makkonen, U., Virkkula, A., Mäntykenttä, J., Hakola, H., Keronen, P., Vakkari, V., & Aalto, P. P.

694         (2012). Semi-continuous gas and inorganic aerosol measurements at a Finnish urban site:

695      Comparisons with filters, nitrogen in aerosol and gas phases, and aerosol acidity. *Atmospheric*

696      *Chemistry and Physics*, *12*(12), 5617–5631. https://doi.org/10.5194/acp-12-5617-2012

697      Malaguti, A., Mircea, M., La Torretta, T. M. G., Telloli, C., Petralia, E., Stracquadanio, M., & Berico, M.

698      (2015). Comparison of online and offline methods for measuring fine secondary inorganic ions and

699      carbonaceous aerosols in the central mediterranean area. *Aerosol and Air Quality Research*, *15*(7),

700      2641–2653. https://doi.org/10.4209/aaqr.2015.04.0240

701      Manchanda, C., Kumar, M., Singh, V., Faisal, M., Hazarika, N., Shukla, A., Lalchandani, V., Goel, V.,

702      Thamban, N., Ganguly, D., & Tripathi, S. N. (2021). Variation in chemical composition and sources

703      of PM2.5 during the COVID-19 lockdown in Delhi. *Environment International*, *153*(December

704      2020), 106541. https://doi.org/10.1016/j.envint.2021.106541

705      Minguillón, M. C., Querol, X., Baltensperger, U., & Prévôt, A. S. H. (2012). Fine and coarse PM

706      composition and sources in rural and urban sites in Switzerland: Local or regional pollution?

707      *Science of the Total Environment*, *427–428*, 191–202.

708      https://doi.org/10.1016/j.scitotenv.2012.04.030

709      Nagar, P. K., Singh, D., Sharma, M., Kumar, A., Aneja, V. P., George, M. P., Agarwal, N., & Shukla, S.

710      P. (2017). Characterization of PM2.5 in Delhi: role and impact of secondary aerosol, burning of

711      biomass, and municipal solid waste and crustal matter. *Environmental Science and Pollution*

712      *Research*, *24*(32), 25179–25189. https://doi.org/10.1007/s11356-017-0171-3

713      Nault, B. A., Campuzano-Jost, P., Day, D. A., Guo, H., Jo, D. S., Handschy, A. V., Pagonis, D., Schroder,

714      J. C., Schueneman, M. K., Cubison, M. J., Dibb, J. E., Hodzic, A., Hu, W., Palm, B. B., & Jimenez,

715      J. L. (2020). Interferences with aerosol acidity quantification due to gas-phase ammonia uptake onto

716      acidic sulfate filter samples. *Atmospheric Measurement Techniques*, *13*(11), 6193–6213.

717      https://doi.org/10.5194/amt-13-6193-2020

718      Nicolás, J. F., Galindo, N., Yubero, E., Pastor, C., Esclapez, R., & Crespo, J. (2009). Aerosol inorganic

719      ions in a semiarid region on the Southeastern Spanish mediterranean coast. *Water, Air, and Soil*

720      *Pollution*, *201*(1–4), 149–159. https://doi.org/10.1007/s11270-008-9934-2

721      Nie, W., Wang, T., Gao, X., Pathak, R. K., Wang, X., Gao, R., Zhang, Q., Yang, L., & Wang, W. (2010).

722      Comparison among filter-based, impactor-based and continuous techniques for measuring

723      atmospheric fine sulfate and nitrate. *Atmospheric Environment*, *44*(35), 4396–4403.

724      https://doi.org/10.1016/j.atmosenv.2010.07.047

725     Pakkanen, T. A., & Hillamo, R. E. (2002). Comparison of sampling artifacts and ion balances for a
726         Berner low-pressure impactor and a virtual impactor. *Boreal Environment Research*, *7*(2), 129–140.

727     Pandolfi, M., Querol, X., Alastuey, A., Jimenez, J. L., Jorba, O., Day, D., Ortega, A., Cubison, M. J.,
728         Comerón, A., Sicard, M., Mohr, C., Prévôt, A. S. H., Minguillón, M. C., Pey, J., Baldasano, J. M.,
729         Burkhart, J. F., Seco, R., Peñuelas, J., Van Drooge, B. L., … Szidat, S. (2014). Effects of sources
730         and meteorology on particulate matter in the Western Mediterranean Basin: An overview of the
731         DAURE campaign. *Journal of Geophysical Research*, *119*(8), 4978–5010.
732         https://doi.org/10.1002/2013JD021079

733     Pant, P., Shukla, A., Kohl, S. D., Chow, J. C., Watson, J. G., & Harrison, R. M. (2015). Characterization
734         of ambient PM2.5 at a pollution hotspot in New Delhi, India and inference of sources. *Atmospheric*
735         *Environment*, *109*, 178–189. https://doi.org/10.1016/j.atmosenv.2015.02.074

736     Panteliadis, P., Helmink, H. J. P., Koopman, P. C., Hoonhout, M., Jonge, D. De, & Visser, J. H. (2012).
737         *PM 10 sampling inlets comparison : EPA vs EU*. *12341*(1999), 12341.

738     Park, S. S., Cho, S. Y., Jo, M. R., Gong, B. J., Park, J. S., & Lee, S. J. (2014). Field evaluation of a near-
739         real time elemental monitor and identification of element sources observed at an air monitoring
740         supersite in Korea. *Atmospheric Pollution Research*, *5*(1), 119–128.
741         https://doi.org/10.5094/APR.2014.015

742     Patel, A., Rastogi, N., Gandhi, U., & Khatri, N. (2021). Oxidative potential of atmospheric PM10 at five
743         different sites of Ahmedabad, a big city in Western India. *Environmental Pollution*, *268*, 115909.
744         https://doi.org/10.1016/j.envpol.2020.115909

745     Pathak, R. K., & Chan, C. K. (2005). Inter-particle and gas-particle interactions in sampling artifacts of
746         PM2.5 in filter-based samplers. *Atmospheric Environment*, *39*(9), 1597–1607.
747         https://doi.org/10.1016/j.atmosenv.2004.10.018

748     Peck, J., Gonzalez, L. A., Williams, L. R., Xu, W., Croteau, P. L., Timko, M. T., Jayne, J. T., Worsnop,
749         D. R., Miake-Lye, R. C., & Smith, K. A. (2016). Development of an aerosol mass spectrometer lens
750         system for PM2.5. *Aerosol Science and Technology*, *50*(8), 781–789.
751         https://doi.org/10.1080/02786826.2016.1190444

752     Pope, C. A., Ezzati, M., & Dockery, D. W. (2009). Fine-Particulate Air Pollution and Life Expectancy in
753         the United States. *New England Journal of Medicine*, *360*(4), 376–386.
754         https://doi.org/10.1056/nejmsa0805646

755 Querol, X., Pey, J., Minguillón, M. C., Pérez, N., Alastuey, A., Viana, M., Moreno, T., Bernabé, R. M.,
756     Blanco, S., Cárdenas, B., Vega, E., Sosa, G., Escalona, S., Ruiz, H., & Artíñano, B. (2008). PM
757     speciation and sources in Mexico during the MILAGRO-2006 campaign. *Atmospheric Chemistry*
758     *and Physics*, *8*(1), 111–128. https://doi.org/10.5194/acp-8-111-2008

759 Rai, P., Furger, M., El Haddad, I., Kumar, V., Wang, L., Singh, A., Dixit, K., Bhattu, D., Petit, J. E.,
760     Ganguly, D., Rastogi, N., Baltensperger, U., Tripathi, S. N., Slowik, J. G., & Prévôt, A. S. H.
761     (2020). Real-time measurement and source apportionment of elements in Delhi's atmosphere.
762     *Science of the Total Environment*, *742*. https://doi.org/10.1016/j.scitotenv.2020.140332

763 Rai, P., Slowik, J. G., Furger, M., El Haddad, I., Visser, S., Tong, Y., Singh, A., Wehrle, G., Kumar, V.,
764     Tobler, A. K., Bhattu, D., Wang, L., Ganguly, D., Rastogi, N., Huang, R. J., Necki, J., Cao, J.,
765     Tripathi, S. N., Baltensperger, U., & Prevot, A. S. H. (2021). Highly time-resolved measurements of
766     element concentrations in PM10 and PM2.5: Comparison of Delhi, Beijing, London, and Krakow.
767     *Atmospheric Chemistry and Physics*, *21*(2), 717–730. https://doi.org/10.5194/acp-21-717-2021

768 Rastogi, N., & Sarin, M. M. (2005). Long-term characterization of ionic species in aerosols from urban
769     and high-altitude sites in western India: Role of mineral dust and anthropogenic sources.
770     *Atmospheric Environment*, *39*(30), 5541–5554. https://doi.org/10.1016/j.atmosenv.2005.06.011

771 Rengarajan, R., Sarin, M. M., & Sudheer, A. K. (2007). Carbonaceous and inorganic species in
772     atmospheric aerosols during wintertime over urban and high-altitude sites in North India. *Journal of*
773     *Geophysical Research Atmospheres*, *112*(21), 1–16. https://doi.org/10.1029/2006JD008150

774 Schaap, M., Spindler, G., Schulz, M., Acker, K., Maenhaut, W., Berner, A., Wieprecht, W., Streit, N.,
775     Müller, K., Brüggemann, E., Chi, X., Putaud, J. P., Hitzenberger, R., Puxbaum, H., Baltensperger,
776     U., & Ten Brink, H. (2004). Artefacts in the sampling of nitrate studied in the "iNTERCOMP"
777     campaigns of EUROTRAC-AEROSOL. *Atmospheric Environment*, *38*(38), 6487–6496.
778     https://doi.org/10.1016/j.atmosenv.2004.08.026

779 Sharma, D., & Kulshrestha, U. C. (2014). Spatial and temporal patterns of air pollutants in rural and
780     urban areas of India. *Environmental Pollution*, *195*(2), 276–281.
781     https://doi.org/10.1016/j.envpol.2014.08.026

782 Sharma, S. K., Mandal, T. K., Jain, S., Saraswati, Sharma, A., & Saxena, M. (2016). Source
783     Apportionment of PM2.5 in Delhi, India Using PMF Model. *Bulletin of Environmental*
784     *Contamination and Toxicology*, *97*(2), 286–293. https://doi.org/10.1007/s00128-016-1836-1

785 Shukla, A. K., Lalchandani, V., Bhattu, D., Dave, J. S., Rai, P., Thamban, N. M., Mishra, S., Gaddamidi,
786    S., Tripathi, N., Vats, P., Rastogi, N., Sahu, L., Ganguly, D., Kumar, M., Singh, V., Gargava, P., &
787    Tripathi, S. N. (2021). Real-time quantification and source apportionment of fine particulate matter
788    including organics and elements in Delhi during summertime. *Atmospheric Environment*, *261*(July),
789    118598. https://doi.org/10.1016/j.atmosenv.2021.118598

790 Singh, A., Rastogi, N., Kumar, V., Slowik, J. G., Satish, R., Lalchandani, V., Thamban, N. M., Rai, P.,
791    Bhattu, D., Vats, P., Ganguly, D., Tripathi, S. N., & Prévôt, A. S. H. (2021). Sources and
792    characteristics of light-absorbing fine particulates over Delhi through the synergy of real-time
793    optical and chemical measurements. *Atmospheric Environment*, *252*(March).
794    https://doi.org/10.1016/j.atmosenv.2021.118338

795 Singh, A., Satish, R. V., & Rastogi, N. (2019). Characteristics and sources of fine organic aerosol over a
796    big semi-arid urban city of western India using HR-ToF-AMS. *Atmospheric Environment*,
797    *208*(April), 103–112. https://doi.org/10.1016/j.atmosenv.2019.04.009

798 Singhai, A., Habib, G., Raman, R. S., & Gupta, T. (2017). Chemical characterization of PM1.0 aerosol in
799    Delhi and source apportionment using positive matrix factorization. *Environmental Science and
800    Pollution Research*, *24*(1), 445–462. https://doi.org/10.1007/s11356-016-7708-8

801 Takahama, S., Wittig, A. E., Vayenas, D. V., Davidson, C. I., & Pandis, S. N. (2004). Modeling the
802    diurnal variation of nitrate during the Pittsburgh Air Quality Study. *Journal of Geophysical
803    Research D: Atmospheres*, *109*(16). https://doi.org/10.1029/2003JD004149

804 Tobler, A., Bhattu, D., Canonaco, F., Lalchandani, V., Shukla, A., Thamban, N. M., Mishra, S.,
805    Srivastava, A. K., Bisht, D. S., Tiwari, S., Singh, S., Močnik, G., Baltensperger, U., Tripathi, S. N.,
806    Slowik, J. G., & Prévôt, A. S. H. (2020). Chemical characterization of PM2.5 and source
807    apportionment of organic aerosol in New Delhi, India. *Science of the Total Environment*, *745*.
808    https://doi.org/10.1016/j.scitotenv.2020.140924

809 Tremper, A. H., Font, A., Priestman, M., Hamad, S. H., Chung, T. C., Pribadi, A., Brown, R. J. C.,
810    Goddard, S. L., Grassineau, N., Petterson, K., Kelly, F. J., & Green, D. C. (2018). Field and
811    laboratory evaluation of a high time resolution x-ray fluorescence instrument for determining the
812    elemental composition of ambient aerosols. *Atmospheric Measurement Techniques*, *11*(6), 3541–
813    3557. https://doi.org/10.5194/amt-11-3541-2018

814 USEPAsepa, & Etv. (2012). *Environmental Technology Verification Report Cooper Environmental*

815      *Services LLC † Xact 625 Particulate Metals Monitor*. September 2012.

816      http://cooperenvironmental.com/

817      Viana, M., Chi, X., Maenhaut, W., Cafmeyer, J., Querol, X., Alastuey, A., Mikuška, P., & Večeřa, Z.

818          (2006). Influence of sampling artefacts on measured PM, OC, and EC levels in carbonaceous

819          aerosols in an urban area. *Aerosol Science and Technology*, *40*(2), 107–117.

820          https://doi.org/10.1080/02786820500484388

821      Wang, M., Aaron, C. P., Madrigano, J., Hoffman, E. A., Angelini, E., Yang, J., Laine, A., Vetterli, T. M.,

822          Kinney, P. L., Sampson, P. D., Sheppard, L. E., Szpiro, A. A., Adar, S. D., Kirwa, K., Smith, B.,

823          Lederer, D. J., Diez-Roux, A. V., Vedal, S., Kaufman, J. D., & Barr, R. G. (2019). Association

824          between long-term exposure to ambient air pollution and change in quantitatively assessed

825          emphysema and lung function. *JAMA - Journal of the American Medical Association*, *322*(6), 546–

826          556. https://doi.org/10.1001/jama.2019.10255

827      Wu, W. S., & Wang, T. (2007). On the performance of a semi-continuous PM2.5 sulphate and nitrate

828          instrument under high loadings of particulate and sulphur dioxide. *Atmospheric Environment*,

829          *41*(26), 5442–5451. https://doi.org/10.1016/j.atmosenv.2007.02.025

830      Zhang, D., Shi, G. Y., Iwasaka, Y., & Hu, M. (2000). Mixture of sulfate and nitrate in coastal atmospheric

831          aerosols: Individual particle studies in Qingdao (36°04'N, 120°21'E), China. *Atmospheric*

832          *Environment*, *34*(17), 2669–2679. https://doi.org/10.1016/S1352-2310(00)00078-9

833      Zhang, X., & Mcmurryt, P. H. (1992). EVAPORATIVE LOSSES OF FINE PARTICULATE

834          NITRATES DURING SAMPLING. In *Atmospheric Environment* (Vol. 26, Issue 18).

835

836